Lithos 248–251 (2016) 257–271

Contents lists available at ScienceDirect

Lithos

journal homepage: www.elsevier.com/locate/lithos

Origin of the DUPAL anomaly in mantle xenoliths of Patagonia (Argentina) and geodynamic consequences☆

Maurizio Mazzucchelli [a,d], Anna Cipriani [a,b,*], Christophe Hémond [c], Alberto Zanetti [d], Gustavo Walter Bertotto [e], Carlos Alberto Cingolani [f]

[a] Dipartimento di Scienze Chimiche e Geologiche, Università di Modena e Reggio Emilia, Via Campi, 103, I-41125 Modena, Italy
[b] Lamont–Doherty Earth Observatory, Columbia University, 61 Route 9 W, Palisades, NY 10964, USA
[c] Domaines Océaniques, Institut Universitaire Européen de la Mer, Université de Brest & CNRS, Place Nicolas Copernic, F-29280 Plouzané, France
[d] Istituto di Geoscienze e Georisorse — CNR, U.O.S. di Pavia, Via Ferrata 1, I-27100 Pavia, Italy
[e] INCITAP. UNLPam-CONICET, Calle Uruguay 151, 6300 Santa Rosa, La Pampa, Argentina
[f] Centro de Investigaciones Geológicas, CONICET-Universidad Nacional de La Plata, Calle 1 n. 644, B1900TAC La Plata, Argentina

ARTICLE INFO

Article history:
Received 11 September 2015
Accepted 14 January 2016
Available online 30 January 2016

Keywords:
Mantle xenoliths
Clinopyroxene
Sr–Nd–Pb isotopes
DUPAL
Tres Lagos
Patagonia

ABSTRACT

The sub-continental lithospheric mantle of South America has been known for some time to carry the DUPAL isotope anomaly as seen in volcanics from the Paraná volcanic province. However, this has not allowed discriminating whether the DUPAL anomaly is a primary feature of the mantle source or acquired during the upwelling and emplacement of the primary magmas. We discovered mantle xenoliths from the Tres Lagos location in Patagonia that carry evidence of percolation by metasomatic melts that imparted the DUPAL isotope anomaly signature. We discuss a model that requires four isotope components (LCC, EM2, HIMU and DM) to account for the Sr, Nd and Pb isotope variability of our samples. We propose that upwelling of hot astenosphere during the Miocene could have triggered the melting of the LCC and EM2 components carrying the DUPAL anomaly, previously entrained in the subcontinental mantle by subduction. These ascending melts would have then metasomatised the local SCLM characterised by DMM and HIMU geochemical affinity generating the hybrid DUPAL-bearing mantle sampled by the Tres Lagos xenoliths.

1. Introduction

The DUPAL isotope anomaly, defined by Hart (1984, 1988) by high $^{208}Pb/^{204}Pb$ and $^{207}Pb/^{204}Pb$ for a given $^{206}Pb/^{204}Pb$ relative to the Northern Hemisphere Reference Line (NHRL, deviations expressed as Δ7/4 and Δ8/4, with Δ8/4 > 60), as well as elevated $^{87}Sr/^{86}Sr$ ratios (>0.705). This anonaly was first documented in mid-ocean ridge basalts of the southern hemisphere (Dupré and Allègre, 1983), later observed in continental magmatism in southern America and southern Africa (Hart, 1984) and in basaltic rocks from eastern Asian continent and South China Sea (Smith, 1998 and reference therein) and more recently discovered in basalts from the Gakkel Ridge (Goldstein et al., 2008).

The DUPAL anomaly is assumed to reflect contamination of the asthenospheric mantle by incorporation of continental and/or oceanic lithospheric mantle or crust/sediment. In the Southern Hemisphere, it has been first attributed to contamination of the sub-continental lithospheric mantle (SCLM) by introduction of lower continental crust (LCC) fragments delaminated during the Gondwana break-up (Allègre and Turcotte, 1985). In MORB from the South Atlantic Ridge and along the three Indian ridges it has been ascribed to several components of mantle or crustal reservoirs: to deep subduction recycling into the mantle of pelagic sediments (Weaver, 1991), to shallow processes such as melting of SCLM (Lustrino, 2005; McKenzie and O'Nions, 1983; Tatsumi, 2000) or of granulitic LCC (Mahoney et al., 1996). These two components have been evoked in the most recent literature (Hoernle et al., 2011) as an alternative to the deep origin proposed, for example, by Class and Le Roex (2011) suggesting that the DUPAL signature is an intrinsic geochemical characteristic of the African superplume.

The mechanism responsible for the incorporation of DUPAL components within the upper mantle is still a matter of debate. Three major processes are envisaged:

i. continental break-up with delamination of SCLM and/or LCC (Class and Le Roex, 2006);
ii. mechanical erosion and entrainment of fragments of LCC along the subduction Wadati–Benioff zone (Clift and Vannucchi, 2004; Keppie et al., 2010; Kukowski and Oncken, 2006; Ranero and von Huene, 2000; von Huene and Scholl, 1991) The mechanism of delamination of LCC and SCLM is a process that has been widely recognised along the Andes in Cenozoic settings, as well as in the

☆ This work is dedicated to the memory of Giorgio Rivalenti who discussed this issue with passion, despite the incurable illness that struck him, until the last day of his life.

* Corresponding author at: Dipartimento di Scienze Chimiche e Geologiche, Università di Modena e Reggio Emilia, Via Campi, 103, I-41125 Modena, Italy.
E-mail address: anna.cipriani@unimore.it (A. Cipriani).

http://dx.doi.org/10.1016/j.lithos.2016.01.010
0024-4937/

Brazilian platform in pre-Mesozoic times (Kay and Coira, 2009 and references therein);

iii. thermo-chemical erosion operated by an uprising mantle plume. This mechanism has been proposed in the southern MAR by Class and Le Roex (2011) where the plume Shona mantle plume would have caused the mobilisation and transfer of deep seated DUPAL components (i.e., South African Proterozoic SCLM or LCC detached material) at higher mantle levels and/or into the erupted melts.

Although the existence of the DUPAL isotopic anomaly in the South American SCLM has already been identified in Brazilian continental flood basalt and in Brazilian carbonatites (Hawkesworth et al., 1986; Toyoda et al., 1994), no anomaly has been detected directly in mantle xenoliths, casting doubts over the origin and significance of this anomaly. Indeed, finding the DUPAL signature only in lavas does not allow discriminating whether the DUPAL anomaly is a primary feature of a mantle source or a secondary one acquired during upwelling and emplacement of the primary magmas.

We present the first evidence of lithospheric mantle xenoliths from the Tres Lagos location in Patagonia with a DUPAL anomaly acquired after interaction with uprising melts. We report new Sr, Nd and Pb isotope data of clinopyroxenes (Cpx) from lherzolitic and harzburgitic mantle xenoliths from the Tres Lagos locality (S 49°13′ 41″, W 71°18′ 16″, Fig. 1), out of which three harzurgites clearly exhibit a DUPAL signature.

Unlike intraplate tectonic settings, the long and multistage geological evolution of Patagonia in a convergent geodynamic setting raises the possibility that the subduction process may have had a relevant role in bringing the DUPAL component down to mantle depths. In our model, the primary DUPAL component is represented by old, granulitic lower continental crust, whose partial melting at mantle depths may be triggered by the ascent of hot asthenospheric mantle. In addition, the subduction of volcanic islands produced by intraplate oceanic magmatism with DUPAL affinity may be an additional way to contaminate locally the mantle wedge.

2. Geological framework

The Tres Lagos outcrop (Fig. 1) occurs at the eastern border of the Meseta de la Muerte, a back-arc basaltic plateau located at the western margin of the Deseado Massif representing an old basement with late Mesoproterozoic to late Neoproterozoic rocks (Gorring et al., 1997). It is positioned in correspondence of a post-plateau volcanic centre, where xenoliths occur in pyroclastites and host lavas. The Tres Lagos latitude coincides with the northern limit of the Austral Volcanic Zone (AVZ, Stern and Kilian, 1996), separated from the southernmost Southern Volcanic Zone (SSVZ) by a gap in the arc magmatism between 49° and 46°30′ latitude S. According to Gorring et al. (1997), this gap is consequent to the collision of the Chile Ridge with South America. The resulting triple junction migrated northward during the last 14 Ma and was at the Tres Lagos latitude ~12 Ma ago. The Meseta de la Muerte main plateau lavas were emplaced during the Miocene, whereas the post-plateau magmas during the upper Miocene to Pliocene (Gorring et al., 1997; Ramos, 1989; Ramos and Kay, 1992). Therefore, it is likely that the plateau lavas are contemporary to the ridge collision and that the post-plateau lavas were emplaced after the opening of the slab window (see also Fig. 5 in Gorring et al., 1997).

3. Petrography

The Tres Lagos xenoliths occur as angular, slightly rounded blocks up to 30 cm in size. Petrographic characteristics define two groups. Group 1 includes spinel lherzolites and harzburgites with protogranular to equigranular and porphyroblastic textures with exsolved pyroxenes. Group 2 includes only three spinel harzburgites with secondary granular texture, where pyroxenes are never exsolved. Their modal composition is reported in Table 1.

In Group 1 lherzolite deformation is weak and displayed mainly by kinked olivine. Orthopyroxene frequently occurs as large porphyroblasts containing relics of olivine and sometimes clinopyroxene (TL 45, Fig. 2). Clinopyroxene is generally a major matrix phase, but in sample TL16, it occurs mainly as a clean phase at triple junctions. Both ortho- and

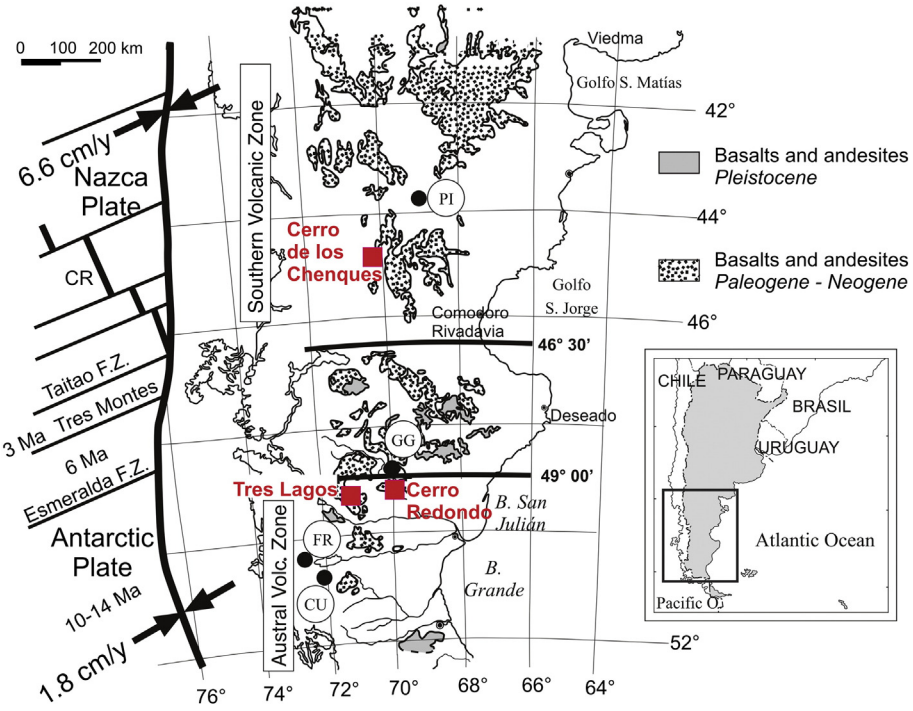

Fig. 1. Sketch map showing the Tres Lagos, Cerro de los Chenques and Cerro Redondo localities and other xenolith occurrences (Circles: PI = Paso de Indios; GG = Gobernador Gregores; FR = El Fraile; CU = Las Cumbres). The two lines at 49° and 46°30′ latitude S limit the gap in the volcanic arc. The map of the plateau and postplateau lavas are from Gorring et al. (1997).

Table 1
Modal composition, textural characteristics, main compositional features of the matrix phases, except of clinopyroxene, and P, T estimates for the Tres Lagos mantle xenoliths.

	Group 1									Group 2		
	Lherzolites						Harzburgite			Harzburgite		
Sample name	TL6	TL13	TL16	TL42	TL45	TL50	TL15	TL66	TL78	TL2	TL8	TL57
Texture	PBL	PBL	PRO	PRO	PBL	EQG	EQG	EQG	EQG	GR-PBL	GR	GR
Clinopyroxene exsolution	Yes	Yes	Yes	Yes	Yes	Yes	Yes	Yes	Yes	No	No	No
Mode												
Olivine	63.6	61.5	67.8	73.0	67.6	68.6	74.6	77.5	77.0	73.2	70.4	84.0
Orthopyroxene	19.3	23.2	24.5	21.3	23.0	15.4	21.4	17.0	18.0	21.4	24.0	14.3
Clinopyroxene	15.2	12.5	6.8	5.0	7.9	13.7	2.8	4.5	4.0	4.9	4.6	0.7
Spinel	1.9	1.7	0.9	0.6	1.4	2.3	1.2	1.0	0.0	0.6	0.9	0.6
Amphibole								tr				
Phlogopite								tr				
Carbonate						tr						
Glass	tr	tr	tr	tr	tr	tr	tr	tr	tr	tr	tr	tr
Olivine												
Fo	91.7	90.2	90.6	90.2	90.2	90.9	89.8	91.1	90.1	91.2	91.3	91.2
CaO	0.10	0.08	0.06	0.07	0.05	0.07	0.03	0.09	0.06	0.06	0.10	0.06
Orthopyroxene												
Mg#	92.2	90.5	91.2	91.2	90.9	91.2	91.1	91.5	91.0	91.3	90.5	92.1
Al_2O_3	5.09	4.65	3.93	3.90	4.17	4.08	2.31	3.88	3.61	3.06	4.20	2.47
TiO_2	0.13	0.14	0.14	0.14	0.11	0.17	0.04	0.07	0.11	0.05	0.13	0.11
Spinel												
Mg#	83.2	77.5	78.0	78.2	78.5	78.0	69.1	73.6	77.0	74.5	75.0	71.0
Cr#	10.4	11.5	15.7	18.0	12.5	17.9	40.8	26.2	18.9	30.3	22.7	43.8
TiO_2	0.15	0.19	0.20	0.19	0.12	0.21	0.10	0.14	0.12	0.10	0.29	0.34
Cr_2O_3	9.9	10.82	14.59	16.45	11.92	16.34	33.07	23.46	17.47	27.51	20.47	36.41
T_{BKN} °C (Brey and Köhler, 1990)	1038	1085	1068	971	1044	1038	1045	1092	1017	997	1123	991
T °C (Taylor, 1998)	975	1013	990	899	972	972	978	1053	932	960	1062	916
$T_{Ca\ in\ Opx}$ °C (Brey and Köhler, 1990)	1000	1006	956	976	955	966	933	1035	949	972	1040	968
T °C (Nimis and Grütter, 2010)	987	994	935	959	933	947	907	1027	927	955	1033	950
P_{Cpx} GPa (Mercier, 1980)	1.8	2.1	2.0	1.7	2.0	1.9	2.2	2.1	2.0	1.8	2.1	1.7
P GPa (Webb and Wood, 1986)	1.8	1.8	1.9	1.9	1.8	1.9	2.2	2.0	1.9	2.1	2.0	2.3

PRO: protogranular; EQG: equigranular; PBL: porphyroblastic; GR: granular.

clinopyroxenes are exsolved. Clinopyroxene, but not orthopyroxene, may present spongy rims (TL6, TL13 and TL45; Fig. 2).

Group 1 harzburgites have always equigranular texture. Orthopyroxene always shows exsolution clinopyroxene lamellae. Clinopyroxene may also be exsolved and occurs at triple junctions or as a minor matrix phase (e.g., TL15). Orthopyroxene substitutes olivine as evidenced by olivine relics within the orthopyroxene. Olivine also shows evidence of re-crystallisation, such as euhedral olivine grown on kinked olivine crystals (Fig. 2). Deformed phlogopite and amphibole occur in sample TL66.

Group 2 harzburgites have granular texture, with 120° triple junctions in sample TL57. Texture may fade into porphyroblastic due to the presence of large olivine and orthopyroxene crystals. Orthopyroxene frequently contains olivine relics and, in sample TL57, exhibits euhedral planes against olivine. Clinopyroxene occurs at triple junctions or in the fine-grained regions of the porphyroblastic domains (e.g., TL2). Pyroxenes are never exsolved. Spinel is always scarce except in sample TL8.

Glass occurs in pockets around amphibole and phlogopite in sample TL66 (Ciuffi, 2002; Ciuffi et al., 2002; Laurora et al., 2001). In all the others xenolith glass occurs as intergranular veins, generally detectable only by SEM examination, but up to 20 to 50 μm in thickness in lherzolites TL6 and TL50 and harzburgites TL8, TL15 and TL50. These veins contain euhedral neocrysts of olivine, clinopyroxene and spinel, and, in TL6 and TL50, also carbonate. As shown in Fig. 2 (TL8), matrix clinopyroxene becomes spongy at the vein contact.

The lavas hosting the xenoliths are vesicular to massive and afiric to porphyric (Stern et al., 1990; Gorring et al., 1997; Gorring and Kay, 2001; this work). The phenocrysts are in order of abundance olivine, plagioclase, clinopyroxene and minor oxides.

4. Analytical methods

Whole rock major elements and Sc, V, Cr, Ni in both mantle xenoliths and host lavas were analysed by X-ray fluorescence spectrometry (XRF), whereas the other trace elements were analysed by inductively coupled plasma-mass spectrometry (ICP-MS).

XRF analyses were carried out at the "Dipartimento di Scienze della Terra dell'Università degli Studi di Modena e Reggio Emilia", Italy, by wavelength dispersive X-ray fluorescence (Philips PW1480) on pressed pellets, using the methods of Franzini et al. (1975) and Leoni and Saitta (1976). Analyses are considered accurate within 2–5% for major elements, and better than 10% for trace elements. The total iron oxide content is reported as FeO.

ICP-MS analyses were carried out at the Department of Earth Sciences of the Memorial University of Newfoundland, St. John's, Newfoundland, Canada. The analytical procedure was as follows: (1) a HF/HNO_3 (+ boric and oxalic acids) digestion of a 0.1 g sample aliquot, (2) analysis of the solution by ICP-MS, using the method of standard addition to correct for matrix effects. Full details of the procedure are given in Jenner et al. (1990). For quality control, two geological reference standards (the gabbro CCRMP MRG-1 and the basalt NIST SRM 688) were prepared and analysed with the samples, together with a reagent blank to measure the reagent contribution to the trace element values. Reagent blank concentrations were insignificant for all the samples and have not been subtracted from sample concentrations. For most elements, the accuracy of the method (1 r.s.d.), determined from multiple analyses of the reference standards, is 3–7%.

Mineral major element analyses for all samples were carried out at the "Dipartimento di Scienze della Terra dell'Università degli Studi di Modena e Reggio Emilia", Italy, with an ARL-SEMQ electron microprobe

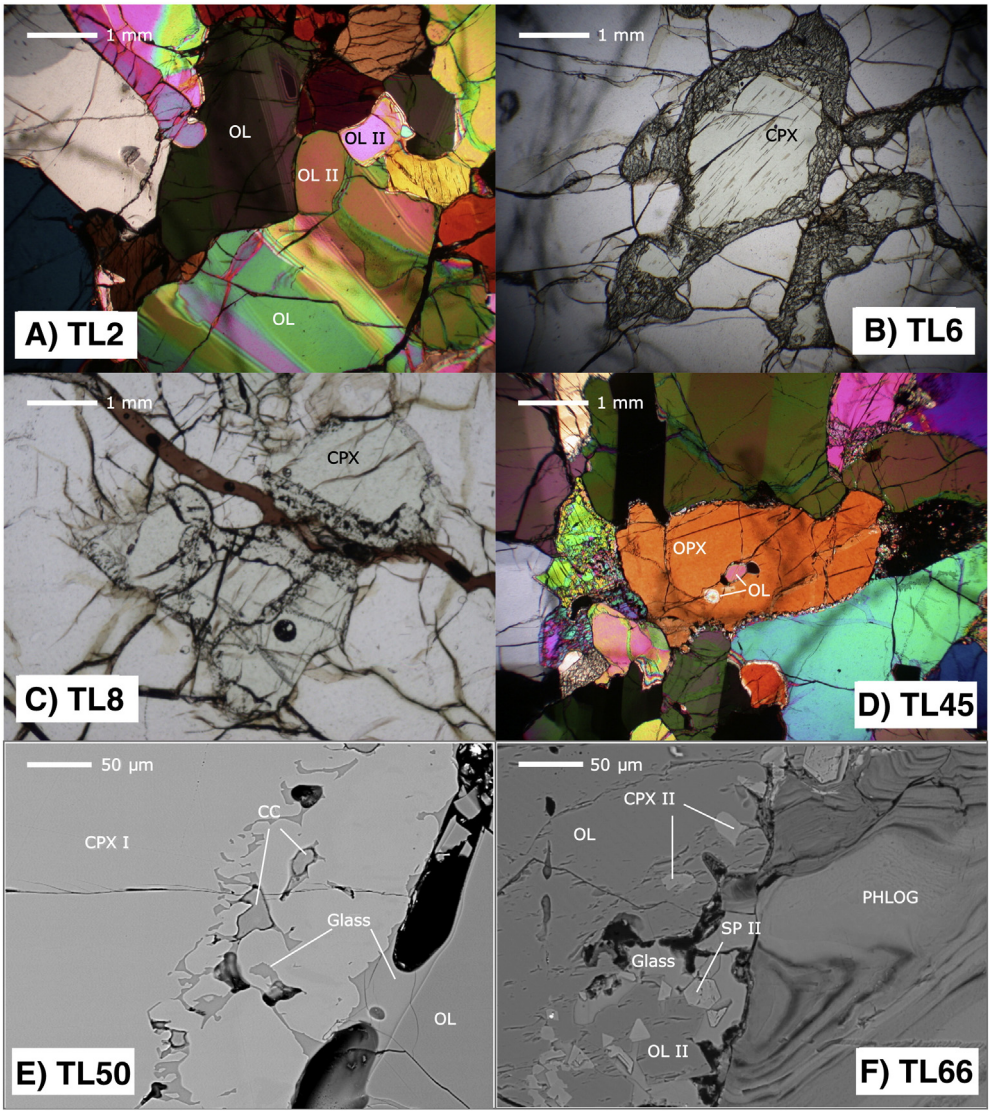

Fig. 2. A: Group 2 harzburgite with porphyroblastic texture. Re-crystallised olivine (OL II) grown on kinked olivine crystals (OL). B: Group 1 lherzolite. Clinopyroxenes (CPX) with spongy rims. C: matrix clinopyroxene spongy at glass vein contact. D: Group 1 lherzolite. Orthopyroxene shows evidence of substitution on olivine, which occurs as relics inside orthopyroxene. Besides in pockets around amphibole and phlogopite in TL66 (F — suggestive of decompression melting, Laurora et al., 2001), in all the xenoliths glass occurs as intergranular veins, generally detectable only by SEM. Only in lherzolites TL6 and TL50 and harzburgites TL8, TL15 and TL50 they are 20 to 50 µm thick. These veins (F) contain euhedral neocrysts of olivine (OL II), clinopyroxene (CPX II) and spinel (SP II), and in TL86 and TL50 (E) also carbonate (CC).

in wavelength dispersive mode, with an accelerating potential of 15 kV, a beam current of 20 nA, and a focused spot size of about 4 µm. Natural minerals were used as standards. Counts were converted to weight percent oxides using the PROBE software by J.J. Donovan (Advanced Microbeam 4217 C, Kings Graces Road, Vienna OH 44473, USA). Results are considered accurate within 2–6%.

Trace elements in clinopyroxenes were analysed by laser ablation-inductively coupled plasma-high resolution mass spectrometry (LA-ICP-HRMS) at the "Istituto di Geoscienze e Georisorse-CNR, Unit of Pavia", consisting of a double-focusing sector-field analyser (Finnigan Mat, Element I) spectrometer coupled with a Q-switched Nd:YAG laser source (Quantel, Brilliant). The fundamental emission of this laser (1064 nm) was converted to 266 nm by two harmonic generators. Helium was used as carrier gas, mixed with Ar downstream of the ablation cell. The spot diameter was 50–60 µm. NIST SRM 610 glass was used as an external standard, with ^{44}Ca as the internal standard. Routine analyses consisted of 1 min background acquisition and 1 min of sample ablation. Precision and accuracy, both better than 10% for concentrations at the ppm level, were assessed from repeated analyses of NIST SRM 612 and BCR-2g standards.

Pb, Nd and Sr isotope ratios of Tres Lagos xenoliths and basalts were measured on clinopyroxene separates and powders, respectively. The clinopyroxenes were carefully checked under a binocular microscope to avoid spinels and sulphides, usually present at the spongy border. Given the careful preparation of our Cpx samples, avoiding any sulphides and spinels, we consider the Pb budget of the clinopyroxenes reflecting the one of their primary sources. We note here also that Mundl et al (2015) did not observe primary sulphides within the clinopyroxene crystals of his Tres Lagos xenoliths. Clinopyroxenes were strongly leached with a solution of 6.2N HCl and 5% HF. Lava powders were leached warm for 1 h with 6N HNO_3. Pb was separated using AG1-X8 anion resin, Sr was separated using Eichrom Sr resin and Nd was separated in a two-column procedure using Eichrom TRU-spec resin to separate the REE, followed by alfa-hydroxy isobutyric acid.

The Sr, Nd and Pb isotopic compositions, and Sm, Nd, Sr and Pb concentrations by isotope dilution, were measured on a VG Sector 54 multicollector thermal ionisation mass spectrometer at the Lamont Doherty Earth Observatory of Columbia University. The $^{143}Nd/^{144}Nd$ and $^{87}Sr/^{86}Sr$ ratios were normalised to an $^{86}Sr/^{88}Sr$ ratio of 0.1194 and $^{146}Nd/^{144}Nd$ ratio of 0.7219, respectively, and reported relative to the La Jolla Nd standard $^{143}Nd/^{144}Nd = 0.511860$ and NBS987 $^{87}Sr/^{86}Sr = 0$ 0.710248. Samples and duplicates were analysed during the course of three analytical sessions. Repeated measurements of the NBS987 Sr standard during the 3 sessions yielded $^{87}Sr/^{86}Sr$ of 0.710270 ± 0.000018 (2σ, N = 17, 25 ppm external reproducibility), of 0.710264 ± 0.000018 (2σ, N = 25, 25 ppm), of 0.710269 ± 0.000012 (2σ, N = 5, 17 ppm). Repeated measurements of the La Jolla Nd standard during the three sessions yielded $^{143}Nd/^{144}Nd$ of 0.511845 ± 0.000012 (2σ, N = 9, 24 ppm external reproducibility), of 0.511841 ± 0.000012 (2σ, N = 8, 24 ppm), of 0.511849 ± 0.000014 (2σ, N = 5, 27 ppm).

Lead isotopes data were collected in static mode using a $^{207}Pb/^{204}Pb$ double spike. Samples and duplicates were analysed during the course of three analytical sessions. For the Tres Lagos xenoliths, measurements of unspiked–double-spiked pairs of the NBS 981 standard were replicated to 177, 243 and 257 ppm (2-s.d. external reproducibility, $n = 52$) for $^{206}Pb/^{204}Pb$, $^{207}Pb/^{204}Pb$ and $^{208}Pb/^{204}Pb$ ratios, respectively. For the CD clinopyroxene measurements of unspiked–double-spiked pairs of the NBS 981, the $^{206}Pb/^{204}Pb$, $^{207}Pb/^{204}Pb$ and $^{208}Pb/^{204}Pb$ ratios were replicated to 172, 221 and 252 ppm (2-s.d. external reproducibility, $n = 50$), respectively. For the TL basalt measurements of unspiked–double-spiked pairs of the NBS 981, the $^{206}Pb/^{204}Pb$, $^{207}Pb/^{204}Pb$ and $^{208}Pb/^{204}Pb$ ratios were replicated to 154, 220, and 166 ppm (2-s.d. external reproducibility, $n = 11$), respectively. These measured Pb isotope ratios were corrected to the Todt et al. (1996) values of 16.9356, 15.4891, and 36.7006, respectively, for NBS 981.

5. Geochemistry

5.1. Xenolith mineral phases

5.1.1. Major elements

Selected chemical parameters of the mineral phases are reported in Table 1, with the full dataset reported in Rivalenti et al. (2004a). Clinopyroxene mineral data are fully reported in Table 2.

Olivine of Group 1 harzburgites has Fo content comparable to those of Group 1 lherzolites. Group 1 harzburgites have orthopyroxenes with lower Al_2O_3 and TiO_2 (Fig. 3) and spinel with lower Mg# (molar Mg / (Mg + Fe) * 100) and TiO_2 and higher Cr# (molar Cr / (Cr + Al) * 100) than those of Group 1 lherzolites (Fig. 3). The major element mineral chemistry of Group 2 harzburgites is essentially similar to that one of Group 1 harzburgites, except for the highest Cr_2O_3 concentration of Group 2 clinopyroxenes (Table 2), the highest TiO_2 concentration of TL8 and TL57 spinels (Fig. 3) and the slightly enriched Fo of Group 2 olivines (Fig. 3). Temperatures and pressures calculated with various geothermobarometers (Table 1) show similar variations for both xenolith groups, indicating provenance from the same lithospheric mantle depths. An extensive discussion about the precision and accuracy of the geothermometers used in Table 1 is reported in Nimis and Grütter (2010). Equilibrium pressure for the peridotites has been inferred according to the geobarometer of Mercier (1980) that gives the best estimates for spinel-facies peridotites (see discussion in Yang et al., 1998). Estimates of the maximum equilibration pressure were calculated using the spinel composition and the empirical equation of Webb and Wood (1986).

5.1.2. Cpx trace elements

Trace element normalised patterns of clinopyroxenes from Group 1 lherzolites (Fig. 4a, c) are homogenously flat in HREE, with abundances slightly higher than 10 xCI (CI from Lyubetskaya and Korenaga, 2007; Fig. 4c). The LREE are slightly depleted in protogranular lherzolites TL16 and TL42, as well as in equigranular lherzolite TL50, whereas they show more complex and variable behaviour in the porphyroblastic lherzolites TL6, TL13 and TL45. In particular, TL6 and TL13 clinopyroxenes show an inversion of the pattern slope in the La–Ce region, with development of a typical spoon-shaped pattern in TL13 lherzolite. Distinctly, the TL45 Cpx is strongly L/MREE-enriched, with La abundance of 100 xCI. The porphyroblastic lherzolites TL6 and TL13 Cpx show enrichments in Th and U, and positive Sr anomaly (Fig. 4a). The highest Th, U and Sr abundances are shown by TL45 clinopyroxenes, whose patterns are also characterised by pronounced negative HFSE anomalies (Fig. 4a).

Clinopyroxenes from Group 1 equigranular harzburgites (Fig. 4a, c) have lower HREE abundances (except for Yb and Lu in TL78) than Group 1 lherzolite (from 9 down to 5 xCI; Fig. 4c). The HREE patterns are flat or characterised by a small positive slope. LREE are slightly depleted (TL15, TL 66) to strongly enriched, with development of a spoon-shaped pattern in sample TL78. The latter clinopyroxenes are also characterised by positive Sr anomaly and relatively large U and Th abundances (Fig. 4a).

Unlike Group 1 clinopyroxenes, the REE patterns of the clinopyroxenes from Group 2 harzburgites (Fig. 4d) have a marked negative slope from MREE to HREE, with Lu 5–6 xCI. TL2 and TL57 clinopyroxenes show humped REE patterns with LREE/MREE << 1. Conversely, TL8 Cpx is strongly enriched in LREE (Fig. 4d), as well as in U, Th, Ta, Nb and Sr (Fig. 4b). An inversion of the pattern slope in correspondence of Ce is shown by TL57 Cpx (Fig. 4d), associated with relatively high U and Th contents, positive Sr anomaly and a prominent positive Zr (and Hf) anomaly (Fig. 4b).

5.1.3. Cpx isotopes

The clinopyroxenes of Tres Lagos xenoliths plot into three well distinct groups in the Sr vs Nd isotope diagram (Table 2 and Fig. 5). Group 1 lherzolite clinopyroxenes show $^{87}Sr/^{86}Sr$ ratios ranging from 0.702293 to 0.702929 and $^{143}Nd/^{144}Nd$ ratios ranging from 0.513025 to 0.513216, with porphyroblastic lherzolite clinopyroxenes TL13 and TL45 being the most enriched in radiogenic Sr and unradiogenic Nd. As a whole, they define a short trend departing from the DMM mantle component towards the Group 1 harzburgite clinopyroxenes, that show, on average, slightly more higher $^{87}Sr/^{86}Sr$ and lower $^{143}Nd/^{144}Nd$ values ($^{87}Sr/^{86}Sr$ ranges from 0.703347 to 0.703561 and $^{143}Nd/^{144}Nd$ from 0.512911 to 0.513025).

All clinopyroxenes of Group 1 xenoliths define an array that plots exactly together with the Chile Ridge basalts trend. Moreover, Group 1 harzburgite clinopyroxenes plot close to the Patagonian plateau basalts field and the Nazca volcanic islands. The $^{207}Pb/^{204}Pb$ and $^{208}Pb/^{204}Pb$ ratios of Group 1 lherzolite and harzburgite clinopyroxenes plot together lying on and slightly above the NHRL (Table 3 and Fig. 6).

Group 2 harzburgite clinopyroxenes have the highest $^{87}Sr/^{86}Sr$ and lowest $^{143}Nd/^{144}Nd$ values of the Tres Lagos xenoliths with $^{87}Sr/^{86}Sr$ ranging from 0.705067 to 0.706487 and $^{143}Nd/^{144}Nd$ ranging from 0.512466 to 0.512664 (Table 2 and Fig. 5). They plot together with the Etendeka and Paraná basalts and are associated with unradiogenic Pb isotope compositions ($^{206}Pb/^{204}Pb = 17.37$-$17.83$, $^{207}Pb/^{204}Pb = 15.55$–$15.60$, $^{208}Pb/^{204}Pb = 37.33$–$38.48$, $^{87}Sr/^{86}Sr = 0.705067$–$0.706487$). The Sr and Pb isotopic ratios of Group 2 harzburgite clinopyroxenes fall within the group of extreme DUPAL samples of Class and Le Roex (2011) and match the values defining the original DUPAL isotope anomaly (Fig. 5, Fig. 6 and Table 3).

In the Pb–Sr isotope space, clinopyroxenes from Cerro de los Chenques mantle xenoliths (Rivalenti et al., 2007a), analysed in an attempt to discover more Patagonian xenoliths with a DUPAL signature, plot within the Patagonian plateau basalts field and close to the Tres Lagos Group 1 lherzolite and harzburgite clinopyroxens (Fig. 5). We note here that Cerro Redondo (S 49°07′ 23″, W 70°08′ 39″, Fig. 1) xenoliths analysed by Schilling et al. (2005) lie between our DUPAL and non-DUPAL xenoliths, therefore showing a DUPAL flavour never identified before.

Table 2
Major, trace element and Sr and Nd isotope compositions for the clinopyroxene of the Tres Lagos mantle xenoliths.

	Group 1									Group 2		
	Lherzolite						Harzburgites			Harzburgites		
Sample name	TL6	TL13	TL16	TL42	TL45	TL50	TL15	TL66	TL78	TL2	TL8	TL57
SiO_2	52.33	52.40	52.64	52.48	52.92	52.40	53.55	52.48	53.18	53.18	52.17	53.43
TiO_2	0.58	0.59	0.60	0.55	0.47	0.67	0.15	0.20	0.49	0.14	0.41	0.46
Al_2O_3	6.57	6.78	6.25	5.97	6.51	5.99	4.77	4.77	6.06	3.90	5.86	4.11
Cr_2O_3	0.75	0.77	0.94	1.16	0.88	0.86	1.06	1.07	1.05	1.46	1.17	1.60
FeO	2.01	2.71	2.37	1.93	2.64	2.20	2.25	2.66	2.16	2.35	2.94	2.10
MnO	0.08	0.10	0.08	0.05	0.09	0.07	0.07	0.10	0.06	0.09	0.09	0.09
MgO	15.58	15.44	15.69	15.12	15.67	15.82	16.65	16.67	15.23	16.27	16.45	15.96
CaO	19.97	19.08	19.39	20.00	19.73	20.01	19.99	20.08	19.38	20.81	19.26	20.38
Na_2O	1.65	1.81	1.78	1.88	1.87	1.55	1.62	1.05	2.12	1.21	1.45	1.63
Sum	99.51	99.70	99.74	99.14	100.78	99.56	100.12	99.10	99.75	99.41	99.81	99.76
Si	1.885	1.888	1.896	1.895	1.889	1.890	1.922	1.911	1.914	1.934	1.883	1.931
Ti	0.016	0.016	0.016	0.015	0.013	0.018	0.004	0.005	0.013	0.004	0.011	0.012
Al	0.279	0.288	0.265	0.254	0.274	0.255	0.202	0.205	0.257	0.167	0.249	0.175
Cr	0.021	0.022	0.027	0.033	0.025	0.025	0.030	0.031	0.030	0.042	0.033	0.046
Fe^{3+}	0.013	0.008	0.007	0.024	0.029	0.012	0.029	0.006	0.007	0.000	0.031	0.006
Fe^{2+}	0.061	0.082	0.071	0.058	0.050	0.066	0.039	0.075	0.065	0.071	0.058	0.063
Mn	0.002	0.003	0.002	0.001	0.003	0.002	0.002	0.003	0.002	0.003	0.003	0.003
Mg	0.837	0.830	0.842	0.814	0.834	0.851	0.891	0.905	0.817	0.882	0.885	0.860
Ca	0.771	0.737	0.748	0.774	0.754	0.773	0.769	0.784	0.747	0.811	0.745	0.789
Na	0.115	0.127	0.124	0.132	0.130	0.108	0.113	0.074	0.148	0.085	0.102	0.114
Mg#	93.2	91.0	92.2	93.3	91.4	92.8	92.9	91.8	92.6	92.5	90.9	93.1
Ba		0.250	0.018		0.130	0.469		0.271		0.686	0.181	1.869
Th	0.142	0.229	0.025	0.012	1.445	0.017	0.024	0.052	0.377	0.019	0.472	0.286
U	0.080	0.052	0.019	0.004	0.375	0.007	0.036	0.018	0.095	0.010	0.133	0.092
Nb	0.616	1.381	0.064	0.042	2.627	0.091		0.145		0.288	2.773	0.305
Ta	0.038	0.021	0.009	0.025	0.140	0.010		0.019	0.011	0.038	0.193	0.035
La	1.37	2.51	1.14	1.32	11.5	0.72	0.29	0.54	6.1	0.59	5.0	1.08
Ce	4.5	5.5	4.7	4.7	30	3.4	0.9	1.9	10	2.4	11	2.4
Pr	0.771	0.850	0.904	0.964	3.893	0.754	0.156	0.349	1.17	0.532	1.48	0.427
Sr	82	101	80	76	240	65	12	28	167	57	147	79
Nd	3.6	4.6	5.0	6.2	15.6	4.4	1.02	1.86	5.0	3.3	6.4	3.5
Hf	0.979	0.993	1.37	1.52	1.14	1.06	0.250	0.514	0.938	0.226	1.44	2.51
Zr	26	33	44	56	40	26	5.6	15	31	12	45	58
Sm	1.72	1.96	1.99	2.26	3.6	1.90	0.340	0.734	1.36	1.22	1.89	1.91
Eu	0.729	0.766	0.822	0.852	1.24	0.728	0.200	0.257	0.512	0.455	0.678	0.764
Gd	2.77	2.62	2.69	3.1	3.5	2.70	0.624	1.04	2.11	1.48	1.98	2.82
Tb	0.443	0.479	0.502	0.529	0.572	0.466	0.174	0.208	0.355	0.230	0.357	0.453
Ti	4228	3166	3487	3772	2526	4489	840	1023	3455	896	2329	2267
Dy	3.4	3.2	3.4	3.6	3.6	3.2	1.26	1.56	2.44	1.57	2.21	2.91
Y	19	20	19	19	22	17	8.3	8.8	14	9.4	13	14
Ho	0.724	0.722	0.691	0.710	0.776	0.699	0.253	0.332	0.575	0.365	0.463	0.539
Er	2.20	2.12	1.90	2.14	2.03	1.98	0.929	1.03	1.56	0.962	1.27	1.38
Tm	0.299	0.298	0.279	0.310	0.315	0.296	0.132	0.146	0.222	0.136	0.178	0.207
Yb	2.01	1.96	1.81	1.97	1.91	1.84	0.919	1.05	1.64	0.872	1.15	1.13
Lu	0.316	0.255	0.241	0.256	0.260	0.248	0.119	0.130	0.258	0.122	0.147	0.114
Sc	65	65	67	72	69	77	70	60	82	69	56	79
V	255	266	287	241	284	290	204	227	250	252	241	216
Cr	4889	8766	10311	7102	9708	5823	9134	8243	7758	9169	12027	10472
$^{87}Sr/^{86}Sr$	0.702293	0.702709	0.702567	0.702457	0.702929	0.702526	0.703347	0.703513	0.703361	0.705480	0.706487	0.705067
2σ	0.000008	0.000007	0.000007	0.000006	0.000007	0.000007	0.000007	0.000007	0.000007	0.000008	0.000006	0.000007
Sr_{ID}	70.5	75.0	63.2	65.5	138.9	49.6	24.7	22.6	137.7	47.1	106.2	74.8
Sm_{ID}	1.665	1.854	1.826	1.788	2.990	2.219	0.402	0.418	1.416	0.952	2.246	1.728
Nd_{ID}	4.358	5.524	4.842	5.269	13.640	4.905	1.090	1.182	4.823	2.928	8.528	3.355
$^{147}Sm/^{144}Nd$	0.2311	0.2029	0.2280	0.2052	0.1325	0.2736	0.2232	0.2137	0.1775	0.1966	0.1592	0.3113
$^{143}Nd/^{144}Nd$	0.513201	0.513047	0.513092	0.513080	0.512946	0.513216	0.512913	0.512911	0.513025	0.512553	0.512664	0.512466
2σ	0.000009	0.000010	0.000008	0.000007	0.000008	0.000008	0.000017	0.000008	0.000006	0.000006	0.000008	0.000010

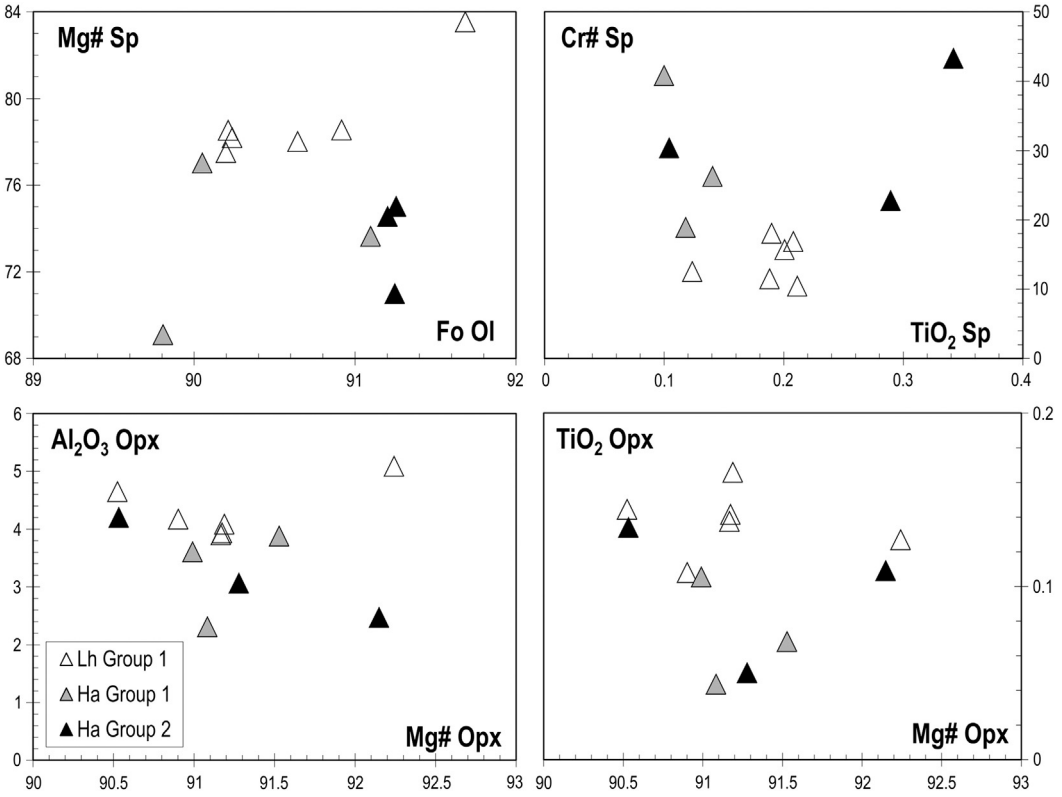

Fig. 3. Selected major element variation trends in olivine–spinel (A), spinel (B) and orthopyroxene (C-D). Mg# = molar Mg / (Mg + Fe) * 100 and Cr# = molar Cr / (Cr + Al) * 100.

5.2. Hosting lava

Compositions of the lavas hosting the Tres Lagos xenoliths vary from basanite to alkali basalt. Normative nepheline ranges from 3.2 to 12.5 (assuming $Fe_2O_3/FeO = 0.15$) and the Mg# values from 61.8 to 68.3. Trace element spidergrams in Fig. 7 show a strongly fractionated REE pattern ($La_n/Yb_n = 17.7–23.1$), high Nb and Ba content ($Nb_n/La_n = 1.7–2.6$, $Ba_n/La_n = 1.2–3.8$), Pb depletion relative to Ce and Nd, positive Sr and minor Ti spikes, and Th enrichment with respect to U. These are common OIB-like characteristics found in back arc basalts that do not carry geochemical components from the subducted slab (cratonic basalts, Stern et al., 1990).

The Sr, Nd and Pb isotope compositions of 4 selected lavas are strongly homogeneous and plot systematically within the Patagonian plateau basalt field; even more remarkably, their Pb isotopic composition is identical to that one of the subducted sediments represented by Leg 141 drill holes. The $^{87}Sr/^{86}Sr$ and $^{143}Nd/^{144}Nd$ ratios of the lavas are clearly distinct from the two groups of xenoliths, but plotting closer to Group 1 lherzolites and harzburgites, towards lower radiogenic Nd and slightly higher radiogenic Sr isotope. The Pb isotopic composition falls within the range of Group 1 lherzolites and harzburgites (Table 4).

The major element composition of the phenocrysts of the host lavas of Tres Lagos and Cerro de los Chenques xenoliths are reported by Ciuffi (2002) and Ciuffi et al. (2002) and their variability reflects typical melt/host reaction between the basalt and xenoliths or xenocrysts.

6. Discussion

Previous studies indicated that the Patagonian (SCLM) records ancient melting-related depletion (Bertotto et al., 2013; Bjerg et al., 2005; 2009; Ntaflos et al., 2007; Rivalenti et al., 2004a) and/or re-fertilisation by later metasomatic processes (Ponce et al., 2015; Rivalenti et al., 2004a). According to several studies, most xenoliths display clear evidence of contamination by slab-derived components from the subducted Pacific oceanic crust (Faccini et al., 2013; Kilian and Stern, 2002; Kilian et al., 1998; Rivalenti et al., 2004a; 2007a). Xenoliths of the farthest occurrences from the arc, such as the Gobernador Gregores outcrop, have been associated to carbonatitic metasomatism (Gorring and Kay, 2000) and/or CO_2-bearing hydrous fluids (Laurora et al., 2001; Rivalenti et al., 2004b).

Geochemical and isotopic evidences in our clinopyroxenes from the Tres Lagos xenoliths re-enforce the major role played by metasomatism in Patagonia and show an unexpected heterogeneity in the lithospheric mantle wedge never sampled before by Patagonian xenoliths. First, we will briefly discuss the processes responsible for the geochemical characteristics of the Group 1 lherzolites and harzburgites. Then, we will extensively discuss the required components to justify the features of Group 2 harzburgites and the origin of their DUPAL anomaly.

6.1. Group 1 lherzolites

Several lines of evidence, i.e., the high Fe content of olivines and pyroxenes, the Al content of pyroxenes and spinel, the Na content of clinopyroxene, the moderate LREE depletion of TL16, TL42 and TL50, and the isotope composition of clinopyroxenes TL6, TL16, TL42 and TL50 (characterised by high Nd and low Sr and Pb isotopic ratios), suggest that Group 1 lherzolites document the occurrence of an enriched DM (E-DMM as defined by Workman and Hart, 2005) reservoir located at lithospheric mantle depths beneath the Tres Lagos area. This observation is consistent with the conclusion of Ntaflos et al. (2007) about the presence of relatively unaltered mantle in this area. In Patagonia, the occurrence of a DM reservoir has been documented in the lithospheric mantle column of Cerro de los Chenques outcrop, located about 200 km east of the Southern Volcanic Zone (SSVZ), further north of the presumed slab window.

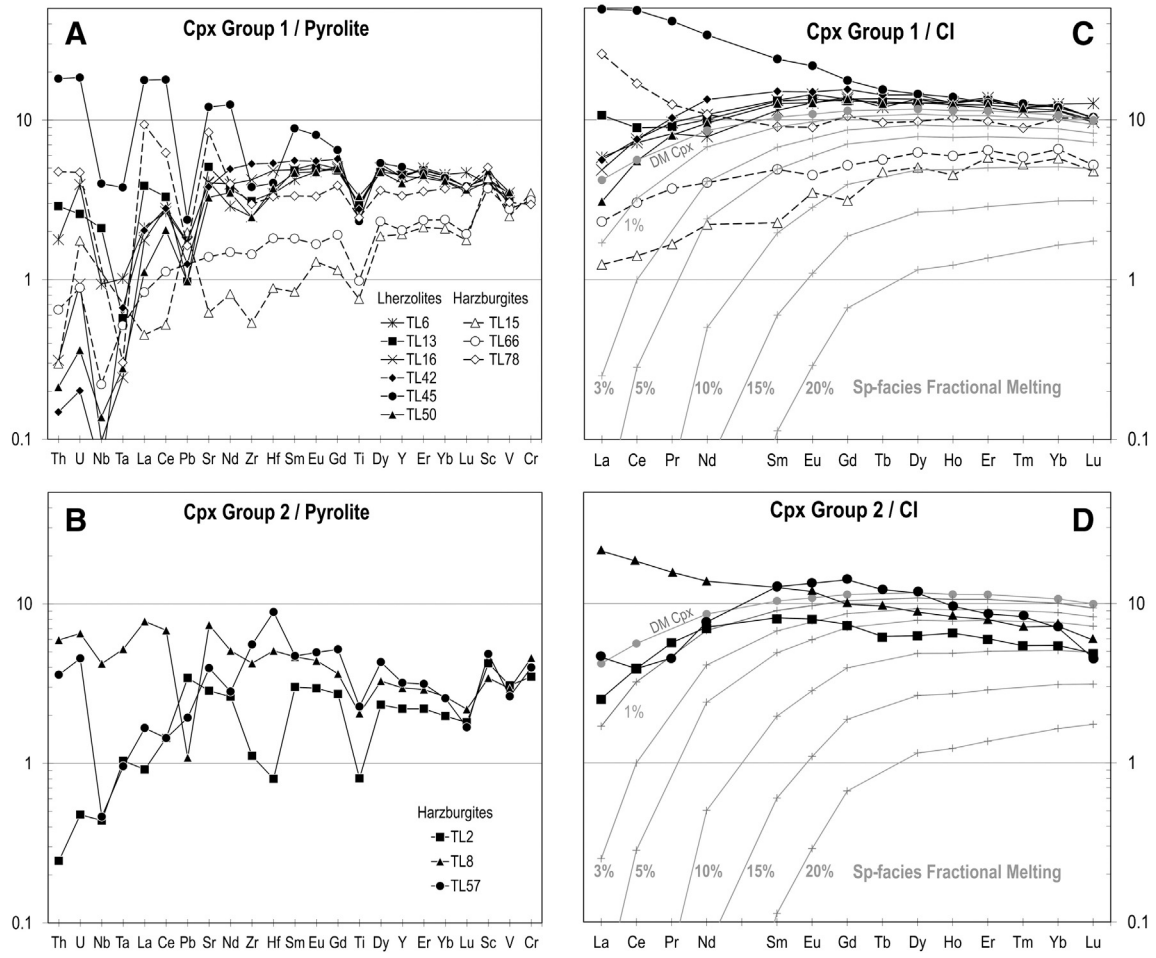

Fig. 4. A, B = clinopyroxene spidergrams normalised to pyrolite composition of Mc Donough and Sun (1995), C, D = clinopyroxene REE patterns, normalised to CI composition of Lyubetskaya and Korenaga (2007), for the lherzolites and harzburgites of Group 1 and harzburgites of Group 2. The chondrite-normalised REE abundance calculated for model clinopyroxene after variable degrees of spinel-facies fractional melting of DMM are reported for comparison in C and D. Details of the fractional melting modelling are reported by Piccardo et al. (2007).

The development of porphyroblastic textures and the Cpx trace element and isotopic compositions of the TL13 and TL45 lherzolites suggest that the Group 1 lherzolite reservoir has been partially metasomatised by small volumes of melts extremely enriched in highly incompatible elements. Clinopyroxenes from TL45 record these enriched compositions, with selective enrichments in U, Th, Sr and LREE (e.g., TL13 sample), which may be attributed to melt–peridotite reaction controlled by ion-exchange chromatographic-type processes in low-porosity mantle (Ionov et al., 2002; Rivalenti et al., 2007a,b; Vernières et al., 1997; Xu et al., 1998). The isotopic composition of these two lherzolites hints at the presence of a HIMU component in the percolating melts (Fig. 6). The presence of a HIMU component in the metasomatic melts is also consistent with the observation that Group 1 lherzolites in the $^{143}Nd/^{144}Nd$ vs $^{87}Sr/^{86}Sr$ diagram (Fig. 6) define a trend lying below the field including the possible mixing lines (see Fig. 6 caption for details on mixing equation) between the compositions of the DM reservoir and the plateau to post-plateau lavas of the adjacent Meseta de la Muerte.

6.2. Group 1 harzburgites

Group 1 harzburgites show a strongly modified reservoir compared with Group 1 lherzolites. The Cpx HREE contents and fractionation are consistent with 3 to 10% of near-fractional melting at spinel-facies conditions of a DM reservoir (to be considered as conservative estimates; Fig. 4). Details of the modelling are reported in Piccardo et al. (2007).

However, the LREE/HREE ratios are too high at a given HREE abundance to be consistent with closed-system partial melting trends. The open-system process is confirmed by the Cpx Sr, Nd and Pb isotopic compositions, which approach that one of the host basalts, and point towards the plateau basalt field. Thus, we propose that Group 1 harzburgites may record the thermo-chemical erosion of the SCLM mantle column beneath the Tres Lagos area driven by the Cenozoic plateau and/or post-plateau magmatism.

6.3. Group 2 harzburgites

The petrographic features and the overall Cpx trace element and isotopic composition of Group 2 harzburgites emphasise a strong recrystallisation and a complete reset of the geochemical budget after porous flow melt migration by high time-integrated melt/rock ratio.

The humped REE patterns with negative slope in the MREE–HREE region shown by Cpx TL2 and TL57 are consistent with Cpx segregation from rather primary melts, like the recrystallised P-type xenoliths of Xu et al. (1998).

Consistently with Group 1 samples, the selective enrichments in U, Th, La, Ce and Sr shown by Cpx TL57 reveal the occurrence of small volumes of late migrating melts enriched in highly incompatible elements. The prominent Zr and Hf positive anomaly of this Cpx is coupled with

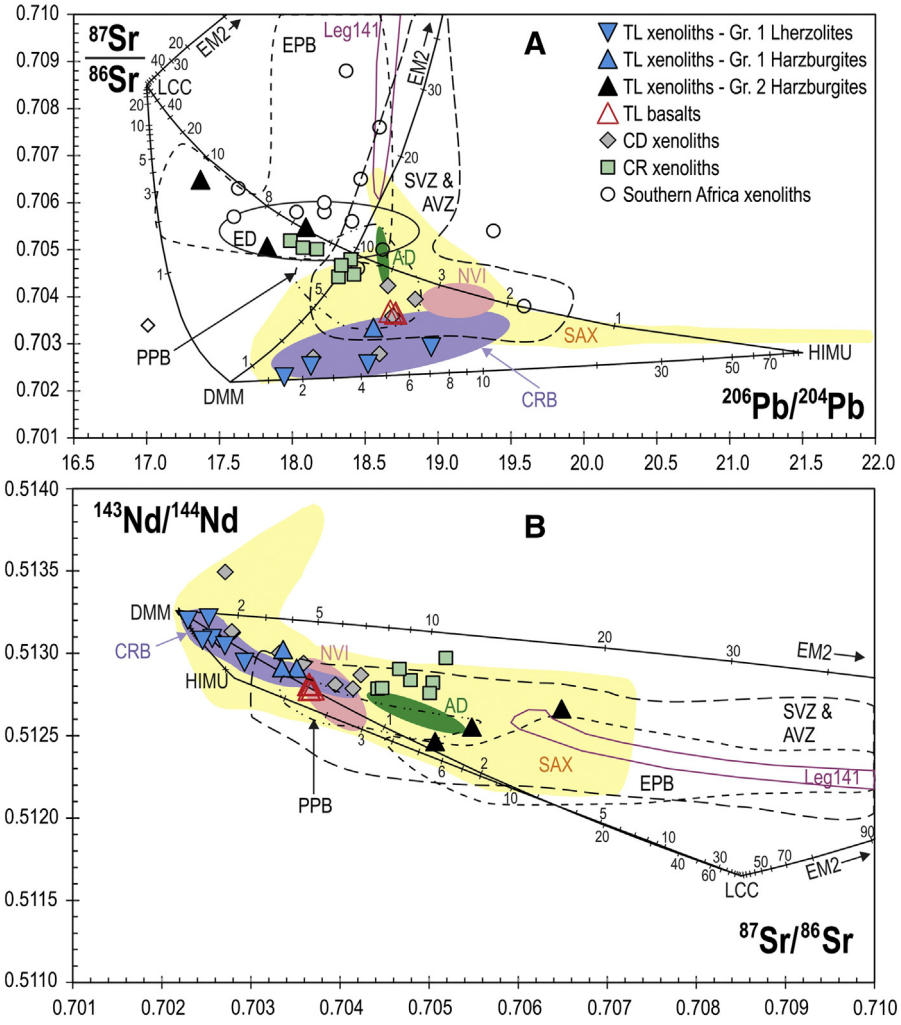

Fig. 5. Simple binary mixing model in (A) the $^{87}Sr/^{86}Sr$ versus $^{206}Pb/^{204}Pb$ space and (B) the $^{143}Nd/^{144}Nd$ versus $^{87}Sr/^{86}Sr$ space between a D-DMM end-member, HIMU end-member, a lower continental crust component and EM2 component according to the mixing equation of Langmuir et al. (1978). The end-member composition is reported in Table 5. Southern America arc volcanics, plateau volcanics, Paraná volcanics and xenoliths are from GEOROC database (georoc.mpch-mainz.gwdg.de) and from Kempton et al. (1999a, 1999b), Schilling et al. (2005), Rivalenti et al. (2007a), Mundl et al. (2015); South African xenoliths and extreme DUPAL field from Class and Le Roex (2011); and Etendeka basalts from Ewart et al. (2004). Chile Ridge basalts from Klein and Karsten (1995). Leg 141 sediments from Kilian and Behrmann (2003). Nazca island basalts from Gerlach et al. (1986). Adakites from Kay et al. (1993) and Stern and Kilian (1996). AD = adakites, AVZ = Austral Volcanic Zone, CRB = Chile Ridge basalts, ED = extreme DUPAL, EPB = Etendeka and Paraná basalts, Leg 141 = Leg 141 sediments, NVI = Nazca volcanic islands, PPB = Patagonian plateau basalts, SAX = Southern America xenoliths, SVZ = Southern Volcanic Zone.

Table 3
Pb isotopic data of the clinopyroxene from the Tres Lagos and Cerro de los Chenques mantle xenoliths.

	Tres Lagos Group 1					Tres Lagos Group 2			Cerro de los Chenques				
	Lherzolite				Harzburgite	Harzburgite							
Sample name	TL6	TL16	TL45	TL50	TL15	TL2	TL8	TL57	CD15	CD18	CD28	CD34	CD61
Pb ID	0.080	0.127	0.141	0.413	0.555	0.156	0.071	0.079					
$^{206}Pb/^{204}Pb$	17.9455	18.5202	18.9532	18.1277	18.5560	18.0930	17.3700	17.8266	18.6564	18.5986	18.8433	18.6873	18.1432
2σ	0.0018	0.0013	0.0014	0.0011	0.0006	0.0045	0.0037	0.0035	0.0014	0.0037	0.0013	0.0034	0.0039
Re-run		18.5163	18.9487		18.5561		17.3662						
2σ		0.0011	0.0014		0.0006		0.0034						
$^{207}Pb/^{204}Pb$	15.4248	15.5637	15.5923	15.5035	15.5716	15.5854	15.5521	15.6040	15.5687	15.5977	15.6192	15.4976	15.5384
2σ	0.0015	0.0012	0.0015	0.0009	0.0005	0.0043	0.0034	0.0037	0.0012	0.0032	0.0010	0.0027	0.0035
Re-run		15.5578	15.5832		15.5718		15.5434						
2σ		0.0009	0.0014		0.0005		0.0034						
$^{208}Pb/^{204}Pb$	37.2893	38.0325	38.7795	37.8124	38.3053	37.9354	37.3383	38.4767	38.4779	38.5420	38.6886	38.4958	38.1922
2σ	0.0036	0.0033	0.0053	0.0023	0.0012	0.0132	0.0089	0.0119	0.0032	0.0080	0.0026	0.0065	0.0086
Re-run		38.0232	38.7680		38.3058		37.3285						
2σ		0.0024	0.0041		0.0012		0.0086						
D8/4 (Hart, 1984)	−3.38	1.46	23.8	26.9	24.4	43.4	71.1	129.7	29.5	42.9	28.0	27.6	63.0

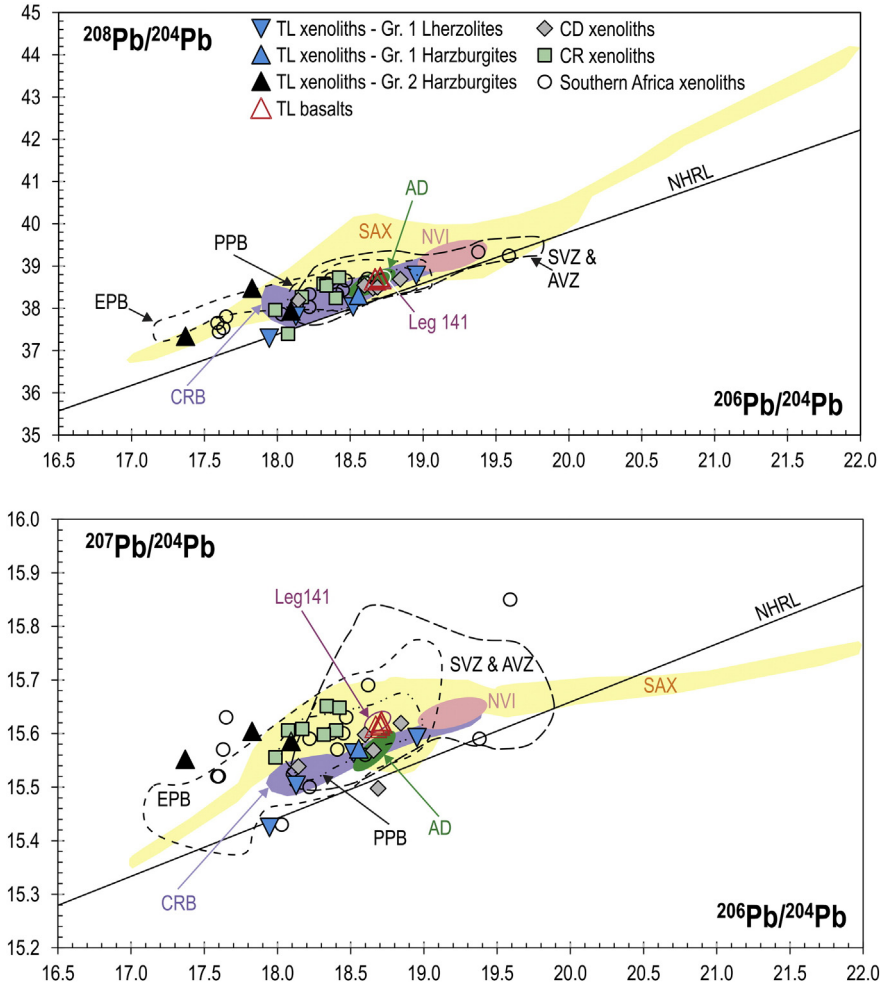

Fig. 6. $^{208}Pb/^{204}Pb$ and $^{207}Pb/^{204}Pb$ versus $^{206}Pb/^{204}Pb$ diagram for the clinopyroxene of Tres Lagos lherzolites and harzburgites of Group 1, harzburgites of Group 2, Tres Lagos basalts and clinopyroxene of Cerro de los Chenques. Southern America arc volcanics, plateau volcanics, Paraná volcanics and xenoliths are from GEOROC database (georoc.mpch-mainz.gwdg.de) and from Rivalenti et al. (2007a), Schilling et al. (2005), Kempton et al. (1999a, 1999b); South African xenoliths from Class and Le Roex (2011); and Etendeka basalts from Ewart et al. (2004). Chile Ridge basalts from Klein and Karsten (1995). Leg 141 sediments from Kilian and Behrmann (2003). Nazca island basalts from Gerlach et al. (1986). Adakites from Kay et al. (1993) and Stern and Kilian (1996). NHRL from Hart (1984). AD = adakites, AVZ = Austral Volcanic Zone, CRB = Chile Ridge basalts, EPB = Etendeka and Paraná basalts, Leg 141 = Leg 141 sediments, NVI = Nazca volcanic islands, PPB = Patagonian Plateau basalts, SAX = Southern America xenoliths, SVZ = Southern Volcanic Zone.

the highest DUPAL anomaly (D8/4 = ~130, Table 3) of the Tres Lagos xenoliths. This may reflect the greatest contribution of the LCC component in the mantle column sampled by TL57 xenolith. Similar Zr and Hf anomalies have been found in cumulitic clinopyroxenites from mantle xenoliths from Bou Ibalrhatene (Middle Atlas, Morocco; Raffone et al., 2009) and in Fe-wehrlites from Tok (Ionov et al., 2006) and have been attributed to Cpx crystallisation from typical alkaline melts. In addition, mantle xenoliths from Kapfenstein also show clinopyroxenes with such anomalies, which have been interpreted as imparted by migration of slab-derived adakitic melts (Coltorti et al., 2007). The composition of the possible late migrating melts in TL xenoliths is potentially recorded by Cpx TL8, with high contents of U, Th, Ta, Nb, LREE and Sr. The observation that Cpx TL8 shows only modest HFSE anomalies (and, in particular, large Nb and Ta contents), suggests that their peculiar composition could be alternatively ascribed to the entrapment of very small volumes of migrating melts rather than superimposed or distinct metasomatic events, as demonstrated by simple numerical simulations (Ionov et al., 2002, 2006; Raffone et al., 2009).

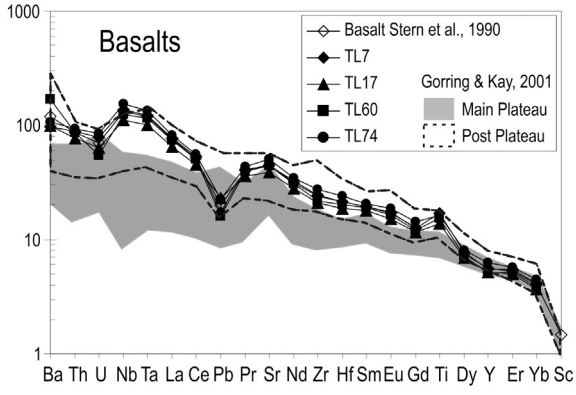

Fig. 7. Basalt spidergrams, for comparison are reported the TL basalt composition of Stern et al. (1990) and the main plateau and post-plateau basalt composition of Gorring and Kay (2001).

The percolating melt (p-melt), estimated only for sample TL2, given its primary melt characteristics, is presented in Fig. 8a and compared with possible melt sources. The p-melt has been calculated based on Cpx trace element concentration and appropriate Cpx/melt partition coefficients using the partition data set of Green et al. (2000) for hydrous basalts at 2 GPa and 1080 °C (consistent with the temperature range of the xenoliths and their spinel facies) and of Hauri et al. (1994) for Th, U and Pb. Hydrous components of the metasomatic agents are suggested by the relic presence of amphibole and phlogopite in one of the samples.

Table 4
Major, trace element and Sr, Nd and Pb isotope composition for the host basalts of the Tres Lagos mantle xenoliths.

		TL7	TL17	TL60	TL74
XRF (wt%)					
SiO_2		47.07	47.43	45.55	46.91
TiO_2		3.10	2.58	2.83	3.02
Al_2O_3		13.33	12.00	12.82	12.95
Cr_2O_3		0.04	0.09	0.03	0.03
FeO_{tot}		11.43	10.91	10.26	11.34
MnO		0.17	0.16	0.17	0.17
MgO		10.36	13.18	9.78	10.85
CaO		8.26	8.65	12.82	8.91
Na_2O		3.19	2.46	3.69	2.85
K_2O		1.89	1.58	1.08	1.86
P_2O_5		0.69	0.68	0.83	0.70
Sum		99.52	99.71	99.87	99.59
XRF (ppm)					
Sc		22	20	23	22
V		192	164	131	192
Ni		495	983	336	527
ICP-MS (ppm)	*Det. Limit*				
Rb	0.261	30	28	5.9	36
Sr	0.920	808	704	799	961
Y	0.113	22	20	20	26
Zr	0.213	236	204	211	274
Nb	0.100	85	68	76	99
Mo	0.339	4.8	3.6	0.830	5.4
Ba	2.51	588	595	1012	677
La	0.139	48	40	45	52
Ce	0.127	86	72	81	90
Pr	0.124	10.0	8.6	9.5	10.7
Nd	0.601	39	33	37	42
Sm	0.198	7.5	6.9	7.4	8.0
Eu	0.033	2.533	2.217	2.376	2.735
Gd	0.167	6.4	5.9	6.2	7.5
Tb	0.139	0.832	0.775	0.815	0.881
Dy	0.254	4.9	4.4	4.6	5.2
Ho	0.123	0.842	0.785	0.809	0.899
Er	0.232	2.30	2.10	2.17	2.28
Tm	0.113	0.224	0.262	0.260	0.245
Yb	0.168	1.71	1.52	1.57	1.85
Lu	0.038	0.249	0.221	0.237	0.271
Hf	0.115	5.8	5.0	5.4	6.6
Ta	0.030	4.3	3.5	4.1	4.8
Pb	0.479	3.1	4.0	2.79	3.9
Th	0.024	7.2	6.2	7.0	7.6
U	0.131	1.61	1.30	1.10	1.69
$^{87}Sr/^{86}Sr$		0.703658	0.703694	0.703657	0.703655
2 s		0.000007	0.000007	0.000007	0.000007
$^{143}Nd/^{144}Nd$		0.512806	0.512785	0.512781	0.512812
2 s		0.000011	0.000010	0.000012	0.000011
$^{206}Pb/^{204}Pb$		18.7082	18.6720	18.7032	18.7097
2 s		0.0012	0.0010	0.0011	0.0012
Re-run		18.7092	18.6712	18.7018	18.7061
2 s		0.0018	0.0009	0.0011	0.0015
$^{207}Pb/^{204}Pb$		15.6232	15.6142	15.6176	15.6212
2 s		0.0011	0.0009	0.0012	0.0013
Re-run		15.6212	15.6126	15.6155	15.6136
2 s		0.0019	0.0008	0.0013	0.0020
$^{208}Pb/^{204}Pb$		38.7406	38.6948	38.7168	38.7285
2 s		0.0032	0.0023	0.0040	0.0037
Re-run		38.7422	38.6931	38.7135	38.7193
2 s		0.0053	0.0024	0.0043	0.0065

Table 5
Composition of the end-members used in the simple binary mixing model of Fig. 5.

	$^{87}Sr/^{86}Sr$	Sr	$^{143}Nd/^{144}Nd$	Nd	$^{206}Pb/^{204}Pb$	Pb
D-DMM	0.70219[a]	6.092[a]	0.51326[a]	0.483[a]	17.573[a]	0.014[a]
HIMU	0.702817[b]	32.6[c]	0.51285[d]	3.31[c]	21.5[e]	0.101[c]
LCC	0.7085[f]	348[g]	0.51165[f]	37.4[g]	17.0[f]	4.0[g]
EM2	0.7128[h]	20.04[h]	0.51265[d]	1.14[h]	19.2[b]	0.144[h]

[a] Workman and Hart (2005).
[b] Jackson and Dasgupta (2008).
[c] Dostal et al. (1998).
[d] Armienti and Longo (2011).
[e] Average between (b) and (c).
[f] Janin et al. (2012).
[g] Rudnick and Gao (2003).
[h] Workman et al. (2004).

Well-known features of subduction-related volcanics and of continental magmas are: Nb depletion relative to La (in arc and continental magmas), Th enrichment relative to U (high in the host basalts, relatively lower in the arc basalts), Sr enrichment relative to Nd (high in arc magmas, relatively low in the host and Chile Ridge basalts, very low in continental crust), the enrichment of Pb relative to Ce (high in arc and continental magmas, low in the host and Chile Ridge basalts) and the REE fractionation (higher in the host than in the arc and Chile Ridge basalts). The calculated TL2 p-melt shows LREE enrichment, positive Pb and Sr anomalies, overall matching the trace element distribution of the Patagonian adakite (Fig. 8).

Concerning the isotopic composition of Group 2 harzburgites, the clinopyroxenes data require a minimum of four distinct components to account for their variations. In a $^{87}Sr/^{86}Sr$ versus $^{206}Pb/^{204}Pb$ diagram, we show that a depleted mantle, variably flavoured by a HIMU component can mix with LCC to various extent and explain the isotopic variability not only of our Tres Lagos xenoliths but also of those of Cerro Redondo (Fig. 5). However, in the $^{143}Nd/^{144}Nd$ versus $^{87}Sr/^{86}Sr$ diagram (Fig. 5), these three components are not sufficient to account for the Sr isotope values of the Tres Lagos samples. A radiogenic fourth component (EM2) is required to account for the higher Sr isotope values for a given Nd isotope composition. The petrological and geochemical features of Tres Lagos Group 2 xenoliths indicate that the DUPAL signature in the Patagonian SCLM was acquired through reaction with migrating melts. This means that the mantle region bearing the DUPAL isotopic composition must have melted in order to contaminate the mantle above, sampled later by the post-plateau magmatic activity.

The overlap of the three DUPAL TL xenoliths with the Etendeka and Paraná LIPs tells us that either the SCLM carries the DUPAL or that the SCLM is metasomatised by plume-derived melts which bear the DUPAL signature. We tend to exclude that the SCLM is the carrier of the DUPAL anomaly given that the DUPAL anomaly is only present in the Tres Lagos and Cerro Redondo locations and is not a widespread characteristic of the Patagonian xenoliths.

6.4. Origin of the DUPAL anomaly of Group 2 xenoliths

In the South America realm, unradiogenic Pb compositions are observed in xenoliths from the Precordilleran basement, along with some parts of the westernmost Sierras Pampeanas (Pie de Palo Range), whose protoliths were formed in an oceanic arc–back-arc setting near a continental margin in Mesoproterozoic time and were accreted to the Gondwana possibly in Ordovician time (Kay et al., 1996; Vujovich et al., 2004). Recent oceanographic expeditions have dredged and sampled in situ, by submersible, granitic and gneissic rocks from the walls of rift structures at the Rio Grande Rise (Sager, 2014; Santos et al., 2014). Precambrian gneisses were also reported long ago at drilled sites in the Campos Basin (off-shore Brazil; Asmus, 1982a, 1982b). These findings support the idea that fragments of continental crust can be incorporated as microcontinents during continental rifting in the oceanic lithosphere, to become actively involved in subduction and in mantle melting processes, contributing to the DUPAL anomaly signature of certain magmas.

Similarly, the involvement of Gondwana crustal material, i.e., African LCC, has also been proposed to explain extreme isotopic compositions found in some Indian MORB. Tanzanian granulites were identified as

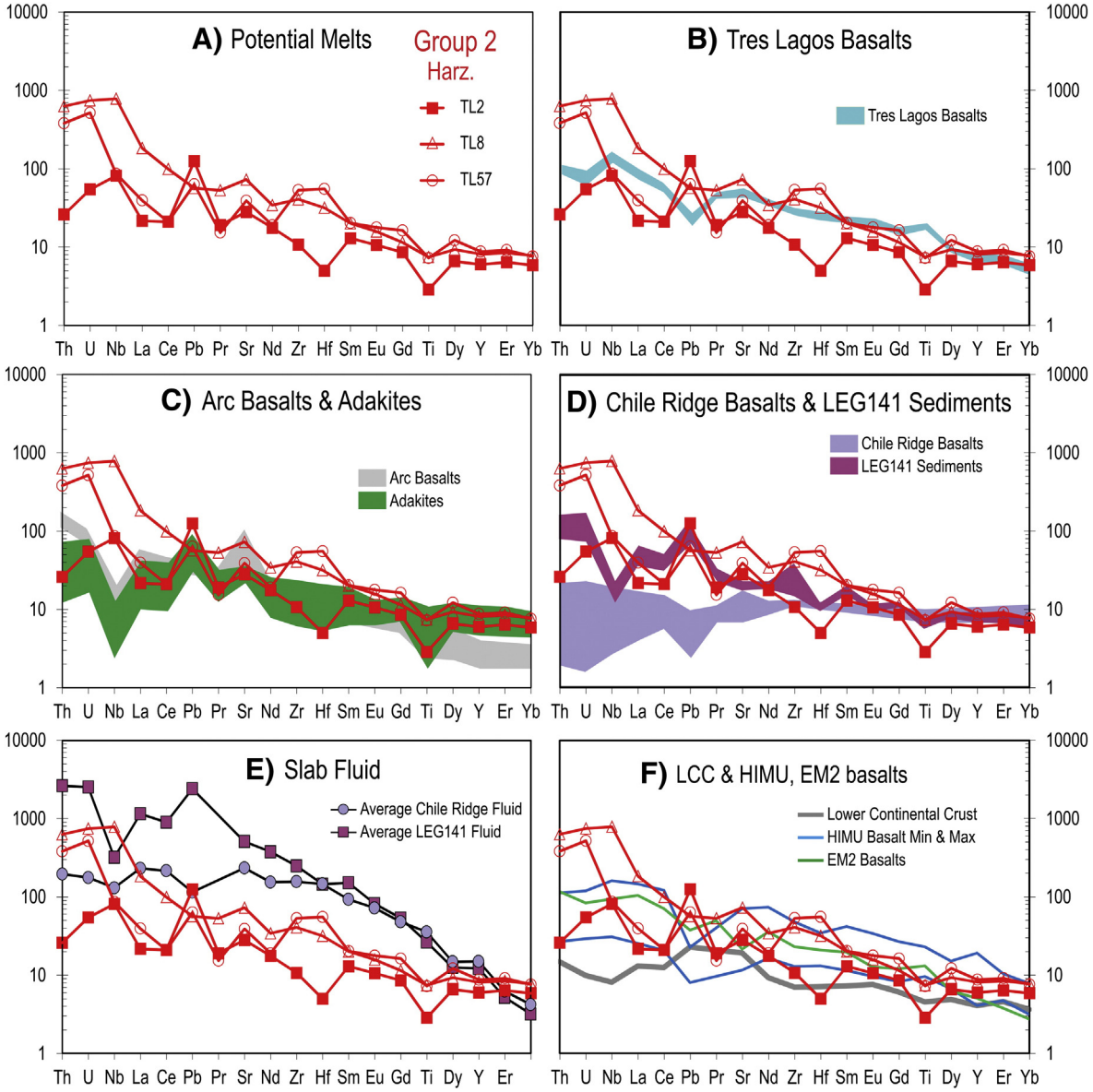

Fig. 8. A = trace element patterns of the melts in equilibrium with clinopyroxene of Group 2 harzburgites normalised to pyrolite composition of Mc Donough and Sun (1995). They are compared with those of: the host basalts (B); arc basalts (D'Orazio et al., 2003; Hickey et al., 1986) and adakites (Kay et al., 1993; Stern and Kilian, 1996) (C); Chile Ridge basalts (Klein and Karsten, 1995; Sturm et al, 1999) and leg 141 sediments (Kilian and Behrmann, 2003) (D); fluids estimated at 4 GPa from Chile Ridge basalts and Leg 141 sediments (Rivalenti et al., 2007a) (E); estimate of lower continental crust (Rudnick and Fountain, 1995), HIMU basalts (Willbold and Stracke, 2010) and the calculated composition of a "Pure" EM2 melt (Workman et al., 2004) (F).

possible sources for these compositions via thermal erosion into the upper mantle during the Gondwana break-up (Janin et al., 2012). Moreover, Class and Le Roex (2011) have proposed the presence of DUPAL components beneath Africa. If such material exists, it might also be present at the base of the South American plate. Indeed, Regelous et al. (2009) mention that the Paraná–Etendeka LIP was centred above the present day DUPAL anomaly of the MAR at about 134 Ma. Such a palaeo-geographic reconstruction (see references in Regelous et al., 2009) would bring Patagonia back above the southern part of the MAR where an elevated DUPAL signal is also recorded in zero-age MORBs. Thus, the DUPAL signature seen in Patagonian magmas could be related to interaction with a comparable LCC component present at the base of the South American plate and mobilised by a mantle plume. Analogous reasoning leads to expect such a component also beneath Antarctica, India and Australia. The LCC component might have been added to the SCLM of Tres Lagos during Meso- to Palaeo-proterozoic time, when it was part of the Rodinia supercontinent, as suggested by the palaeogeographic reconstruction of Mundl et al. (2015). If the introduction of LCC within the upper mantle beneath Tres Lagos occurred through lithosphere delamination during the Gondwana break-up and consequently through lithosphere delamination, that event should be younger than 200 Ma.

Alternatively, the emplacement of LCC could be related to the specific geological setting of Patagonia that is dominated by subduction processes. It could be envisaged that the DUPAL anomaly has been imparted to the SCLM by old subduction of volcanic islands or plateaus, produced by intraplate oceanic magmatism (Gerlach et al., 1986), according to the evidence that subduction episodes occurred in the past below the actual Deseado Massif since the Ordovician (Ramos, 2008; 2009).

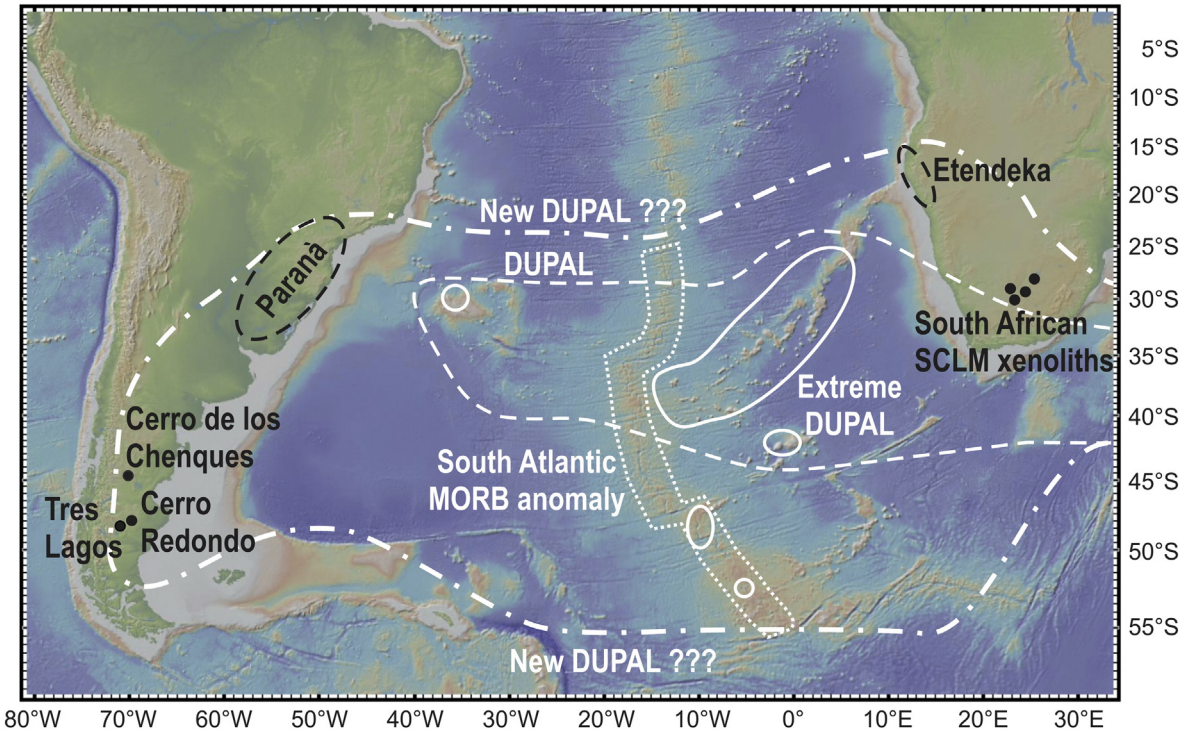

Fig. 9. Present day sketch map illustrating the locations of the Patagonian Tres Lagos, Cerro de los Chenques and Cerro Redondo (Schilling et al., 2005) SCLM occurrences, the locations of the Southern Africa SCLM xenolith occurrences (Class and Le Roex, 2011), the South Atlantic DUPAL anomaly (as drawn by Condie, 2005), the extreme DUPAL and South Atlantic MORB anomaly (Class and Le Roex, 2011). A new wider DUPAL anomaly field is here proposed for the southern hemisphere.

On the other hand, the addition of the DUPAL component could have been accomplished by mechanical erosion of the accretionary prism along the subduction zone of the SW Gondwana margin (Abre et al., 2012) or the Patagonia microcontinent (Ramos, 2008; 2009 and reference therein). In this frame, its age could be much younger, namely Jurassic (i.e., the period when the east-dipping subduction began at this latitude; Giacosa et al., 2012) to Oligocene (according to the present day convergence rates of the Nazca and South America plates and the distance of the Tres Lagos locality from the trench).

The DUPAL signature has been imparted to spinel-facies SCLM peridotites beneath Tres Lagos by interstitial migration of ascending melts, implying that a DUPAL reservoir melted at greater depth. The absence of exsolution lamellae in pyroxenes and of evidence of deformation in the equigranular to porphyroblastic Group 2 harzburgites indicate that the interstitial melt migration imparting the DUPAL signature was the latest process affecting the mantle sequence (if the reaction with the host basalts and the veins intrusion are not taken into account). Moreover, the Tres Lagos area, as well as Cerro Redondo, is located at the transition zone between the Meseta de la Muerte basaltic plateau and the backarc of the Austral Volcanic Zone, presently a "normal" suprasubduction setting. These observations suggest a possible genetic link between the generation of the DUPAL signature in the Tres Lagos Group 2 harzburgites and the Miocene basaltic magmatism of the Meseta de la Muerte plateau. The Meseta de la Muerte area experienced an exceptional thermal perturbation during the Miocene with consequent development of plateau magmatism, which is supposedly related to the development of a slab window. In this frame, the upwelling of the hot asthenosphere during Miocene (independently from the development or not of an actual slab-window) could have triggered the melting of the LCC (and EM2) component with DUPAL anomaly, previously subducted at great depth, beneath the SCLM (with DMM and HIMU geochemical affinity). This could have taken place also in the laterally adjacent, southern part, now represented by the back-arc of the Austral Volcanic Zone, therefore affecting the Tres Lagos and Cerro Redondo localities. The thermal perturbation has probably produced several aliquots of melts with DUPAL anomaly scattered in the plateau basalts. As reported by Folguera and Ramos (2011), the process of shallowing and steepening of the subduction zone could have occurred near the Tres Lagos latitude, with the consequence of facilitating the injection of hot asthenosphere in the sub-continental mantle and lower crust.

The concomitant production of intraplate volcanics with OIB geochemical affinity and post-collisional melts bearing crustal component is a phenomenon observed in other subduction-related settings affected by the uprising of hot asthenosphere (e.g., Alboran domain, Western Mediterranean Region: Rampone et al., 2010 and references therein).

7. Concluding remarks

We conclude that the DUPAL anomaly in the Southern Hemisphere is geographically more extended than previously thought (Fig. 9) and we interpret our observations in support of a model in which uprising mantle melts having EM2 and LCC signatures interacted with a SCLM mantle column with DMM and HIMU geochemical affinity. In this framework, the mobilisation of the LCC granulitic and EM2 components might have been triggered by additional heat delivered by the uprising asthenosphere. We propose that such heat might have been provided by the relatively recent subduction of the Chile Ridge (Tertiary to present) that induced the upwelling of hot asthenosphere during the Miocene (independently from the development or not of an actual slab-window) forming the Meseta de la Muerte basaltic plateau. Asthenospheric melts would then react with and mobilise LCC and EM2 components in the surrounding hot SCLM and produce deeply modified peridotitic bodies that acquire a DUPAL signature, such as those sampled as xenoliths in Tres Lagos.

Acknowledgements

We thank the Facultad de Ciencias Exactas y Naturales (Universidad de La Pampa, Argentina — PI 235), CONICET (PIP 2011-956), CNR–CONICET joint programme (years 2013–2014), and the "Programma Giovani Ricercatori — Rita Levi Montalcini" (to A.C.) for their financial support. The manuscript benefited from constructive reviews by V.A. Ramos and an anonymous reviewer. We thank M.L. Gorring for a stimulating discussion of a previous version of the manuscript. This is Lamont–Doherty Earth Observatory Contribution #7966.

References

Abre, P., Cingolani, C.A., Cairncross, B., Chemale Jr., F., 2012. Siliciclastic Ordovician to Silurian units of the Argentine Precordillera: constraints on provenance and tectonic setting in the proto-Andean margin of Gondwana. Journal of South American Earth Sciences 40, 1–22.

Allègre, C.J., Turcotte, D.L., 1985. Geodynamic mixing in the mesosphere boundary layer and the origin of oceanic islands. Geophysical Research Letters 12, 207–210.

Armienti, P., Longo, P., 2011. Three-dimensional representation of geochemical data from a multidimensional compositional space. International Journal of Geosciences 2, 231–239.

Asmus, H.E., 1982a. Geotectonic significance of Mesozoic–Cenozoic magmatic rocks in the Brazilian continental margin and adjoining emerged area. Quinto Congreso Latinoamericano de Geologia, Buenos Aires, Argentina, October 17th–22nd, 1982. ACTAS 3, 761–779.

Asmus, H.E., 1982b. Caracteristicas estruturais e estratigráficas da margem continental Brasileira como elementos criticos do modelo de sua evolucão. Quinto Congreso Latinoamericano de Geologia, Buenos Aires, Argentina, October 17th–22nd, 1982. ACTAS 3, 781–798.

Bertotto, G.W., Mazzucchelli, M., Zanetti, A., Vannucci, R., 2013. Petrology and geochemistry of the back-arc lithospheric mantle beneath eastern Payunia (La Pampa, Argentina): evidence from Agua Poca peridotite xenoliths. Geochemical Journal 47, 219–234.

Bjerg, E.A., Ntaflos, T., Kurat, G., Dobosi, G., Labudia, C.H., 2005. The upper mantle beneath Patagonia, Argentina, documented by xenoliths from alkali basalts. Journal of South American Earth Sciences 18, 125–145.

Bjerg, E.A., Ntaflos, Th., Thöni, M., Aliani, P., Labudia, C.H., 2009. Heterogeneous lithospheric mantle beneath northern Patagonia: evidence from Prahuaniyeu garnet- and spinel-peridotites. Journal of Petrology 50, 1267–1298.

Brey, G.P., Köhler, T., 1990. Geothermobarometry in four-phase lherzolites. II. New thermobarometers and practical assesment of existing thermobarometers. Journal of Petrology 31, 1353–1378.

Ciuffi, S., 2002. Xenoliti ultramafici di Cerro de Los Chenques (Chubut, Argentina) e Tres Lagos (Santa Cruz, Argentina). Petrologia e geochimica del mantello litosferico in ambiente di retro-arco (Ph.D. Thesis). University of Modena and Reggio Emilia, Modena (189 pp.).

Ciuffi, S., Rivalenti, G., Vannucci, R., Zanetti, A., Mazzucchelli, M., Cingolani, C.A., 2002. Are the glasses in mantle xenoliths witness of the metasomatic agent composition? V. M. Godschmidt Conference, Davos, Switzerland. Conference Abstracts, Special Supplement. Geochimica et Cosmochimica Acta 66 (Abstract #143).

Class, C., Le Roex, A., 2006. Continental material in the shallow oceanic mantle—how does it get there? Geology 34, 129–132.

Class, C., Le Roex, A., 2011. South Atlantic DUPAL anomaly — dynamic and compositional evidence against a recent shallow origin. Earth and Planetary Science Letters 305, 92–102.

Clift, P., Vannucchi, P., 2004. Controls on tectonic accretion versus erosion in subduction zones: implications for the origin and recycling of the continental crust. Reviews of Geophysics 42, 1–31.

Coltorti, M., Bonadiman, C., Faccini, B., Ntaflos, T., Siena, F., 2007. Slab melt and intraplate metasomatism in Kapfenstein mantle xenoliths (Styrian Basin, Austria). Lithos 94, 66–89.

Condie, K.C., 2005. Earth as an Evolving Planetary System. 1st ed. Elsevier Academic Press.

D'Orazio, M., Innocenti, F., Manetti, P., Tamponi, M., Tonarini, S., Gonzàles-Ferran, O., Lahsen, A., Omarini, R., 2003. The quaternary calc-alkaline volcanism of the Patagonian Andes close to the Chile triple junction: geochemistry and petrogenesis of volcanic rocks from the Cay and Maca volcanoes (~45°S, Chile). Journal of South American Earth Sciences 16, 219–242.

Dostal, J., Cousens, B., Dupuy, C., 1998. The incompatible element characteristics of an ancient subducted sedimentary component in ocean island basalts from French Polynesia. Journal of Petrology 39, 937–952.

Dupré, B., Allègre, C.J., 1983. Pb–Sr isotope variation in Indian Ocean basalts and mixing phenomena. Nature 303, 142–146.

Ewart, A., Marsh, J.S., Milner, S.C., Duncan, A.R., Kamber, B.S., Armstrong, R.A., 2004. Petrology and geochemistry of Early Cretaceous bimodal continental flood Volcanism of the NW Etendeka, Namibia. Part 1: introduction, mafic lavas and re-evaluation of mantle source components. Journal of Petrology 45, 59–105.

Faccini, B., Bonadiman, C., Coltorti, M., Gregoire, M., Siena, F., 2013. Oceanic material recycled within the sub-Patagonian lithospheric mantle (Cerro del Fraile, Argentina). Journal of Petrology 54, 1211–1258.

Folguera, A., Ramos, V.A., 2011. Repeated eastward shifts of arc magmatism in the Southern Andes: a revision to the long-term pattern of Andean uplift and magmatism. Journal of South American Earth Sciences 32, 531–546.

Franzini, M., Leoni, L., Saitta, M., 1975. Revisione di una metodologia analitica per fluorescenza-X, basata sulla correzione completa degli effetti di matrice. Rendiconti della Società Italiana di Mineralogia e Petrologia 31, 365–378.

Gerlach, D.C., Hart, S.R., Morales, V.W.J., Palacios, C., 1986. Mantle heterogeneity beneath the Nazca plate: San Felix and Juan Fernandez islands. Nature 322, 165–169.

Giacosa, R., Fracchia, D., Heredia, N., 2012. Structure of the Southern Patagonian Andes at 49°S, Argentina. Geologica Acta 10, 265–282.

Goldstein, S.L., Soffer, G., Langmuir, C.H., Lehnert, K., Graham, D.W., Michael, P.J., 2008. Origin of a 'Southern Hemisphere' geochemical signature in the Arctic upper mantle. Nature 453, 89–93.

Gorring, M.L., Kay, S.M., 2000. Carbonatite metasomatized peridotite xenoliths from southern Patagonia: implications for lithospheric processes and Neogene plateau magmatism. Contributions to Mineralogy and Petrology 140, 55–72.

Gorring, M.L., Kay, S.M., 2001. Mantle processes and sources of Neogene slab window magmas from Southern Patagonia, Argentina. Journal of Petrology 42, 1067–1094.

Gorring, M.L., Kay, S.M., Zitler, P.K., Ramos, V.A., Rubiolo, D., Fernandez, M.I., Panza, J.L., 1997. Neogene Patagonian plateau lavas: continental magmas associated with ridge collision at the Chile Triple Junction. Tectonics 16, 1–17.

Green, T.H., Blundy, J.D., Adam, J., Yaxley, G.M., 2000. SIMS determination of trace element partition coefficients between garnet, clinopyroxene and hydrous basaltic liquids at 2–7.5 GPa and 1080–1200 °C. Lithos 53, 165–187.

Hart, S.R., 1984. A large scale isotope anomaly in the southern hemisphere mantle. Nature 309, 753–757.

Hart, S.R., 1988. Heterogeneous mantle domains: signatures, genesis and mixing chronologies. Earth and Planetary Science Letters 90, 273–296.

Hauri, E.H., Wagner, T.P., Grove, T.L., 1994. Experimental and natural partitioning of Th, U, Pb and other trace elements between garnet, clinopyroxene and basaltic melts. Chemical Geology 117, 149–166.

Hawkesworth, C.J., Mantovani, M.S.M., Taylor, P.N., Palacz, Z., 1986. Evidence from Paraná of south Brazil for a continental contribution to DUPAL basalts. Nature 322, 356–359.

Hickey, R.L., Frey, F.A., Gerlach, D.C., López-Escobar, L., 1986. Multiple sources for basaltic arc rocks from the southern volcanic zone of the Andes (34°–41°S): trace element and isotopic evidence for contributions from subducted oceanic crust, mantle, and continental crust. Journal of Geophysical Research 91, 5963–5983.

Hoernle, K., Hauff, F., Werner, R., van den Bogaard, P., Gibbons, A.D., Conrad, S., Müller, R.D., 2011. Origin of Indian Ocean Seamount Province by shallow recycling of continental lithosphere. Nature Geoscience 4, 883–887.

Ionov, D.A., Bodinier, J.-L., Mukasa, S.B., Zanetti, A., 2002. Mechanisms and sources of mantle metasomatism: major and trace element compositions of peridotite xenoliths from Spitsbergen in the context of numerical modelling. Journal of Petrology 43, 2219–2259.

Ionov, D.A., Chazot, G., Chauvel, C., Merlet, C., Bodinier, J.-L., 2006. Trace element distribution in peridotite xenoliths from Tok, SE Siberian craton: a record of pervasive, multi-stage metasomatism in shallow refractory mantle. Geochimica et Cosmochimica Acta 70, 1231–1260.

Jackson, M.G., Dasgupta, R., 2008. Compositions of HIMU, EM1 and EM2 from global trends between radiogenic isotopes and major elements in ocean island basalts. Earth and Planetary Science Letters 276, 175–186.

Janin, M., Hémond, C., Maia, M., Nonnotte, P., Ponzevera, E., Johnson, K.T.M., 2012. The Amsterdam–St. Paul Plateau: a complex hot spot/DUPAL-flavored MORB interaction. Geochemistry, Geophysics, Geosystems 13, Q09016. http://dx.doi.org/10.1029/2012GC004165.

Jenner, G.A., Longerich, H.P., Jackson, S.E., Fryer, B.J., 1990. ICP-MS — a powerful tool for high-precision trace-element analysis in Earth sciences: evidence from analysis of selected U.S.G.S. reference samples. Chemical Geology 83, 133–148.

Kay, S.M., Coira, B.L., 2009. Shallowing and steepening subduction zones, continental lithospheric loss, magmatism, and crustal flow under the central Andean Altiplano–Puna Plateau. In: Kay, S.M., Ramos, V.A., Dickinson, W.R. (Eds.), Backbone of the Americas: Shallow Subduction, Plateau Uplift, and Ridge and Terrane Collision. Geological Society of America Memoir 204, pp. 229–260. http://dx.doi.org/10.1130/2009.1204(11).

Kay, S.M., Ramos, V.A., Marquez, M., 1993. Evidence in Cerro Pampa volcanic rocks for slab-melting prior to ridge–trench collision in Southern South America. Journal of Geology 101, 703–714.

Kay, S.M., Orrell, S., Abbruzzi, J.M., 1996. Zircon and whole rock Nd–Pb isotopic evidence for a Grenville Age and a Laurentian origin for the basement of the Precordillera in Argentina. The Journal of Geology 104, 637–648.

Kempton, P.D., Hawkesworth, C.J., Lopez-Escobar, L., Ware, A.J., 1999a. Spinel + garnet lherzolite xenoliths from Pali Aike, part 2. Trace element and isotopic evidence bearing on the evolution of lithospheric mantle beneath Southern Patagonia. In: Gurney, J.J., Gurney, G.L., Pascoe, M.D., Richardson, S.H. (Eds.), The J.B. Dawson Volume, Proceedings of the VIIth International Kimberlite Conference. Red Rood Design, Cape Town, pp. 415–428.

Kempton, P.D., Lopez-Escobar, L., Hawkesworth, C.J., Pearson, G., Ware, A.J., 1999b. Spinel + garnet lherzolite xenoliths from Pali Aike, Part 1. Petrography, mineral chemistry and geothermobarometry. In: Gurney, J.J., Gurney, G.L., Pascoe, M.D., Richardson, S.H. (Eds.), The J.B. Dawson Volume, Proceedings of the VIIth International Kimberlite Conference. Red Rood Design, Cape Town, pp. 403–414.

Keppie, J.D., Nance, R.D., Murphy, J.B., Dostal, J., Braide, J.A., 2010. The high-pressure Iberian–Czech belt in the Variscan orogen: extrusion into the upper (Gondwanan) plate? In: Nance, R.D. (Ed.), The Rheic Ocean: Palaeozoic evolution from Gondwana and Laurussia to Pangaea. Gondwana Research 17, pp. 306–316

Kilian, R., Behrmann, J.H., 2003. Geochemical constraints on the sources of Southern Chile trench sediments and their recycling in arc magmas of the Southern Andes. Journal. of the Geological Society, London 160, 57–70.
Kilian, R., Stern, C.R., 2002. Constraints on the interaction between slab melts and the mantle wedge from adakitic glass in peridote xenoliths. European Journal of Mineralogy 14, 25–36.
Kilian, R., Franzen, C., Koch, M., 1998. The metasomatism of the mantle wedge below the southern Andes: constraints from laser ablation microprobe ICP-MS trace element analysis of clinopyroxenes, orthopyroxenes and fluid inclusions of mantle xenoliths. Terra Nostra 98 (5), 82–83.
Klein, E.M., Karsten, J.L., 1995. Ocean–ridge basalts with convergent margin geochemical affinities from the Chile Ridge. Nature 374, 52–57.
Kukowski, N., Oncken, O., 2006. Subduction erosion — the "Normal" mode of fore-arc material transfer along the Chilean Margin? In: Oncken, O., Chong, G., Franz, G., Giese, P., Götze, H.-J., Ramos, V.A., Strecker, M.R., Wigger, P. (Eds.), The Andes: Active Subductive Orogeny. Frontiers in Earth Sciences, Springer, Berlin, pp. 217–236
Langmuir, C.H., Vocke Jr., R.D., Hanson, G.N., 1978. A general mixing equation with applications to Icelandic basalts. Earth and Planetary Science Letters 37, 380–392.
Laurora, A., Mazzucchelli, M., Rivalenti, G., Vannucci, R., Zanetti, A., Barbieri, M.A., Cingolani, C.A., 2001. Metasomatism and melting in carbonated peridotite xenoliths from the mantle wedge: the Gobernador Gregores case (Southern Patagonia). Journal of Petrology 42, 7-69.
Leoni, L., Saitta, M., 1976. X-ray fluorescence analysis of 29 trace elements in rock and mineral standards. Rendiconti della Società Italiana di Mineralogia e Petrologia 32, 497–510.
Lustrino, M., 2005. How the delamination and detachment of lower crust can influence basaltic magmatism. Earth Science Reviews 72, 21–38.
Lyubetskaya, T., Korenaga, J., 2007. Chemical composition of Earth's primitive mantle and its variance: 1. Method and results. Journal of Geophysical Research 112, B03211. http://dx.doi.org/10.1029/2005JB004223.
Mahoney, J.J., White, W.M., Upton, B.G.J., Neal, C.R., Scrutton, R.A., 1996. Beyond EM-1: lavas from Afanasy-Nikitin Rise and the Crozet Archipelago, Indian Ocean. Geology 24, 615–618.
Mc Donough, W.F., Sun, S.-S., 1995. Composition of the Earth. Chemical Geology 120, 223–253.
McKenzie, D., O'Nions, R.K., 1983. Mantle reservoirs and ocean island basalts. Nature 301, 229–231.
Mercier, J.-C.C., 1980. Single-pyroxene thermobarometry. Tectonophysics 70, 1–37.
Mundl, A., Ntaflos, Th., Ackerman, L., Bizimis, M., Bjerg, E.A., Hauzenberger, C.A., 2015. Mesoproterozoic and Paleoproterozoic subcontinental lithospheric mantle domains beneath southern Patagonia: isotopic evidence for its connection to Africa and Antarctica. Geology 43, 39–42.
Nimis, P., Grütter, H., 2010. Internally consistent geothermometers for garnet peridotites and pyroxenites. Contributions to Mineralogy and Petrology 159, 411–427.
Ntaflos, Th., Bjerg, E.A., Labudia, C.H., Kurat, G., 2007. Depleted lithosphere from the mantle wedge beneath Tres Lagos, Southern Patagonia, Argentina. Lithos 94, 46–65.
Piccardo, G.B., Zanetti, A., Müntener, O., 2007. Melt/peridotite interaction in the Southern Lanzo peridotite: field, textural and geochemical evidence. Lithos 94, 181–209.
Ponce, A.D., Bertotto, G.W., Zanetti, A., Brunelli, D., Giovanardi, T., Aragón, E., Bernardi, M.I., Hémond, C., Mazzucchelli, M., 2015. Short-scale variability of the SCLM beneath the extra-Andean back-arc (Paso de Indios, Argentina): evidence from spinel-facies mantle xenoliths. Open Geosciences 7, 362–385.
Raffone, N., Chazot, G., Pin, C., Vannucci, R., Zanetti, A., 2009. Metasomatism in the lithospheric mantle beneath Middle Atlas (Morocco) and the origin of Fe- and Mg-rich wehrlites. Journal of Petrology 50, 197–249.
Ramos, V.A., 1989. Andean Foothills structures in northern Magallanes Basin Argentina. The American Association of Petroleum Geologists Bulletin 73, 887–903.
Ramos, V.A., 2008. Patagonia: a paleozoic continent adrift? Journal of South American Earth Sciences 26, 235–251.
Ramos, V.A., 2009. Anatomy and global context of the Andes: main geologic features and the Andean orogenic cycle. In: Kay, S.M., Ramos, V.A., Dickinson, W.R. (Eds.), Backbone of the Americas: Shallow Subduction, Plateau Uplift, and Ridge and Terrane Collision. Geological Society of America Memoir 204, pp. 31–65.
Ramos, V.A., Kay, S.M., 1992. Southern Patagonian plateau basalts and deformation: backarc testimony of ridge collisions. Tectonophysics 205, 261–282.
Rampone, E., Vissers, R.L.M., Poggio, M., Scambelluri, M., Zanetti, A., 2010. Melt migration and intrusion during exhumation of the Alboran lithosphere: the Tallante mantle xenolith record (Betic Cordillera, SE Spain). Journal of Petrology 51, 295–325.
Ranero, C.R., von Huene, R., 2000. Subduction erosion along the Middle America convergent margin. Nature 404, 748–752.
Regelous, M., Niu, Y., Abouchami, W., Castillo, P.R., 2009. Shallow origin for South Atlantic DUPAL anomaly from lower continental crust: geochemical evidence from the Mid-Atlantic Ridge at 26°S. Lithos 112, 57–72.
Rivalenti, G., Mazzucchelli, M., Laurora, A., Ciuffi, S.I.A., Zanetti, A., Vannucci, R., Cingolani, C.A., 2004a. The backarc mantle lithosphere in Patagonia, South America. Journal of South American Earth Sciences 17, 121–152.
Rivalenti, G., Zanetti, A., Mazzucchelli, M., Vannucci, R., Cingolani, C.A., 2004b. Equivocal carbonatite markers in the mantle xenoliths of the Patagonia backarc: the Gobernador Gregores case (Santa Cruz Province, Argentina). Contributions to Mineralogy and Petrology 147, 647–670.
Rivalenti, G., Mazzucchelli, M., Zanetti, A., Vannucci, R., Bollinger, C., Hémond, C., Bertotto, G.W., 2007a. Xenoliths from Cerro de los Chenques (Patagonia): an example of slab-related metasomatism in the backarc lithospheric mantle. Lithos 99, 45–67.
Rivalenti, G., Girardi, V.A.V., Zanetti, A., Mazzucchelli, M., Tassinari, C.C.G., Bertotto, G.W., 2007b. The effect of the Fernando de Noronha plume on the mantle lithosphere in north-eastern Brazil. Lithos 94, 111–131.
Rudnick, R.L., Fountain, D.M., 1995. Nature and composition of the continental crust: a lower crustal perspective. Reviews of Geophysics 33, 267–309.
Rudnick, R.L., Gao, S., 2003. Composition of the continental crust. In: Holland, H.D., Turekian, K.K. (Eds.), Treatise on Geochemistry vol. 3. Elsevier, Amsterdam, pp. 1–64.
Sager, W.W., 2014. Scientific drilling in the South Atlantic: Rio Grande Rise, Walvis Ridge and surrounding areas Rio de Janeiro, April 2-–5, 2014. U.S. Science Support Program Workshop Report by William W. Sagerp. 13.
Santos, R.V., Glasmacher, U.A., Geldmacher, J., 2014. Scientific drilling in the South Atlanic, IODP Workshop, Rio de Janeiro, Brazil, 2–5 April 2014. EOS, Transactions, American Geophysical Union 95, 249.
Schilling, M.E., Conceicão, R.V., Mallmann, G., Koester, E., Kawashita, K., Hervé, F., Morata, D., Motoki, A., 2005. Spinel-facies mantle xenoliths from Cerro Redondo, Argentine Patagonia: petrographic, geochemical, and isotopic evidence of interaction between xenoliths and host basalt. Lithos 82, 485–502.
Smith, A.D., 1998. The geodynamic significance of the DUPAL anomaly in Asia. In: Martin Flower, M.F.J., Chung, S.-L., Lo, C.-H., Lee, T.-Y. (Eds.), Mantle Dynamics and Plate Interactions in East AsiaGeophysical Monograph 27. American Geophysical Union, Washington, D.C., pp. 89–105.
Stern, C.R., Kilian, R., 1996. Role of the subducted slab, mantle wedge and continental crust in the generation of adakites from the Andean Austral Volcanic Zone. Contributions to Mineralogy and Petrology 123, 263–281.
Stern, C.R., Frey, F.A., Futa, K., Zartman, R.E., Peng, Z., Kyser, T.K., 1990. Trace-element and Sr, Nd, Pb, and O isotopic composition of Pliocene and Quaternary alkali basalts of the Patagonia Plateau lavas of southernmost South America. Contributions to Mineralogy and Petrology 104, 294–308.
Sturm, M.E., Klein, E.M., Graham, D.W., Karsten, J., 1999. Age constraints on crustal recycling to the mantle beneath the southern Chile Ridge: He–Pb–Sr–Nd isotope systematics. Journal of Geophysical Research 105, 5097–5114.
Tatsumi, Y., 2000. Continental crust formation by crustal delamination in subduction zones and complementary accumulation of the enriched mantle I component in the mantle. Geochemistry, Geophysics, Geosystems 1. http://dx.doi.org/10.1029/2000GC000094.
Taylor, W.R., 1998. An experimental test of some geothermometer and geobarometer formulations for upper mantle peridotites with application to the thermobarometry of fertile lherzolite and garnet websterite. Neues Jahrbuch für Mineralogie Abhandlungen 172, 381–408.
Todt, W., Cliff, R.A., Hanser, A., Hofmann, A.W., 1996. Evaluation of a ^{202}Pb–^{205}Pb double spike for high-precision lead isotope analysis. In: Basu, A.R., Hart, S.R. (Eds.), Earth Processes: Reading the Isotopic CodeGeophysical Monograph 95. American Geophysical Union, Washington D.C., pp. 429–437.
Toyoda, K., Horiuchi, H., Tokonami, M., 1994. DUPAL anomaly of Brazilian carbonatites: geochemical correlations with hotspots in the South Atlantic and implications for the mantle source. Earth and Planetary Science Letters 126, 315–331.
Vernières, J., Godard, M., Bodinier, J.-L., 1997. A plate model for thesimulation of trace element fractionation during partial melting and magma transport in the Earth's upper mantle. Journal of Geophysical Research 102, 24771–24784.
von Huene, R., Scholl, D.W., 1991. The return of sialic material to the mantle indicated by terrigeneous material subducted at convergent margins. Tectonophysics 219, 163–175.
Vujovich, G.I., van Staal, C.R., Davis, W., 2004. Age constraints on the tectonic evolution and provenance of the Pie de Palo Complex, Cuyania composite terrane, and the Famatinian Orogeny in the Sierra de Pie de Palo, San Juan, Argentina. Gondwana Research 7, 1041–1056.
Weaver, B.L., 1991. The origin of oceanic island basalt end-member compositions: trace element and isotopic constraints. Earth and Planetary Science Letters 104, 381–397.
Webb, S.A.C., Wood, B.J., 1986. Spinel–pyroxene–garnet relationships and their dependence on Cr/Al ratio. Contributions to Mineralogy and Petrology 92, 471–480.
Willbold, M., Stracke, A., 2010. Formation of enriched mantle components by recycling of upper and lower continental crust. Chemical Geology 276, 188–197.
Workman, R.K., Hart, S.R., 2005. Major and trace element composition of the depleted MORB mantle (DMM). Earth and Planetary Science Letters 231, 53–72.
Workman, R.K., Hart, S.R., Jackson, M., Regelous, M., Farley, K.A., Blusztajn, J., Kurz, M., Staudigel, M., 2004. Recycled metasomatized lithosphere as the origin of the enriched mantle II (EM2) end-member: evidence from the Samoan volcanic chain. Geochemistry, Geophysics, Geosystems 5, Q04008. http://dx.doi.org/10.1029/2003GC000623.
Xu, Y.G., Menzies, M.A., Bodinier, J.L., Bedini, R.M., Vroon, P., Mercier, J.C.C., 1998. Melt percolation–reaction atop the plume: evidence from spinel harzburgite poikiloblastic xenoliths from Boree Massif Central, France. Contribution to Mineralogy and Petrology 132, 65–84.
Yang, H.-J., Sen, G., Shimizu, N., 1998. Mid-Ocean ridge melting: constraints from lithospheric xenoliths at Oahu, Hawaii. Journal of Petrology 39, 277–295.